

A Geometric Theory of Intersymbol Interference

Part I: Zero-Forcing and Decision-Feedback Equalization

By D. G. MESSERSCHMITT

(Manuscript received May 14, 1973)

A linear-space geometric theory of intersymbol interference is introduced in this paper. An equivalence between the structure of intersymbol interference and a wide-sense stationary discrete random process is demonstrated and exploited to demonstrate the equivalence of zero-forcing (decision-feedback) equalization to minimum mean-square error linear interpolation (prediction) of a random process. This equivalence is used to quickly derive the properties of these equalizers and give them additional geometric interpretation. Results from prediction theory are used to develop practical computational methods of determining the tap-gains of the infinite equalizers for both rational and nonrational channel power spectra. Finally, the theory of reproducing kernel Hilbert spaces is used to develop a theory of equalization for nonstationary channels with nonstationary noise.

I. INTRODUCTION

The analysis of digital communication systems from a geometrical viewpoint—the viewing of waveforms as points in a signal space and the identification of cross-correlation with the formation of an inner product—is by now well established. To a large extent, this approach has been popularized by the book of Wozencraft and Jacobs.¹ However, when it comes to analyzing systems with intersymbol interference, frequency-domain techniques have almost exclusively been relied upon. The purpose of this paper is to consider pulse-amplitude modulation (PAM) systems with intersymbol interference from a geometric standpoint, and more specifically to develop a geometric theory of equalization.

Consideration of the geometric structure of intersymbol interference leads immediately to the observation of a striking correspondence to the theory of minimum mean-square error (MMSE) linear estimation of a wide-sense stationary discrete-parameter random process. The fact that the latter subject is almost exclusively treated by geometric methods^{2,3} is further impetus for this approach to equalization.

The theories of linear zero-forcing equalization and decision-feedback equalization are well established. The properties of linear equalization

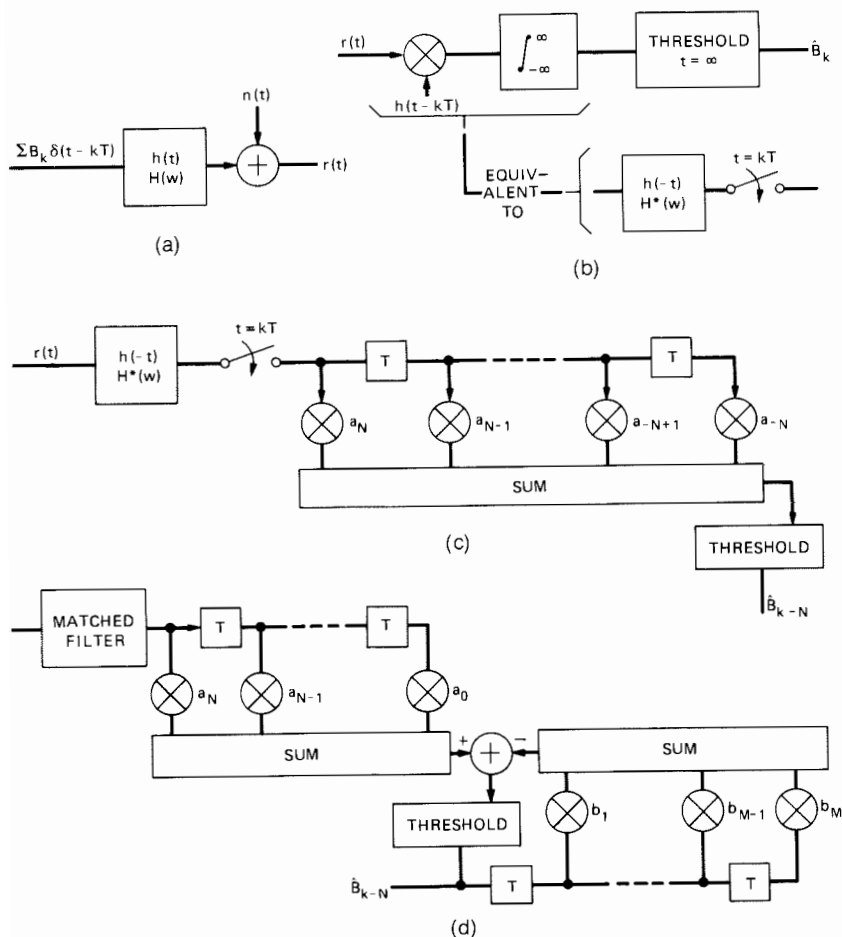


Fig. 1—(a) Communication system model. (b) Matched-filter receiver. (c) Zero-forcing equalizer. (d) Decision-feedback equalizer.

are summarized by Lucky, et al.,⁴ while the present state of knowledge of decision-feedback equalization is summarized by Mosen⁵ and Price.⁶ The primary analysis tools which have been used are the calculus of variations in the case of linear equalization and Toeplitz forms in the case of decision-feedback equalization.

In this paper, the geometric approach enables us to treat the two types of equalization simultaneously using the same mathematical framework, in which the relationship between them becomes very clear and many of their known properties are given an additional geometric interpretation. Many of the results follow directly from the theory of MMSE estimation. In addition to the unification and reinterpretation of previously known results, the geometric approach leads to extensions of the theory in several directions. Among these are the derivation of an orthogonal expansion in Section 2.4 which is useful in many problems involving intersymbol interference, the development of practical iterative techniques for determining equalizer tap-gains (the infinite case) in Section 3.4, the extension of the theory of equalization to nonstationary noise and a time-varying channel in Section IV, and numerous results on the minimum distance problem associated with the performance analysis of the Viterbi algorithm maximum likelihood detector in a companion paper.⁷

This paper together with a companion one⁷ expand upon an earlier talk.⁸ Readers desiring a limited and short treatment of this subject may wish to refer there. The geometrical approach to intersymbol interference was also employed to a limited extent in the author's thesis.⁹

1.1 Problem Statement

We will consider the detection of a sequence of digital data digits, B_k , each assuming one of a finite and predetermined number of levels, from the reception

$$r(t) = \sum_{k=N_1}^{N_2} B_k h(t - kT) + n(t) \quad (1)$$

as determined from the communication system model of Fig. 1a. It will be assumed initially that $n(t)$ is white Gaussian noise (this assumption will be relaxed in Section IV).[†] A simple matched-filter receiver for the reception of $r(t)$ is shown in Fig. 1b. In the first of two equivalent formulations of this receiver, the reception is cross-correlated

[†] The assumption of Gaussian noise is not necessary for the majority of results to follow, and in particular those which involve only second-order statistics of the noise.

with $h(t - kT)$ and the decision on B_k made by applying a series of thresholds to the result; in the second formulation the cross-correlator is realized as a filter with impulse response $h(-t)$ (commonly called a matched filter) whose output is sampled at $t = kT$. The matched-filter receiver is optimum when there is no intersymbol interference, but in the presence of intersymbol interference the matched filter will respond to more than a single data digit and the performance of the receiver will be degraded.

When there is intersymbol interference, a common approach is to build a linear filter, called a zero-forcing equalizer (ZFE), which responds to only a single time-translate of $h(t)$ (this can only be approximated in practice). The most common form of this equalizer, shown in Fig. 1c, is a matched filter followed by transversal filter (MFTF). As $N \rightarrow \infty$ the tap-gains of the transversal filter can be chosen such that the threshold input is a function of only a single data digit. It is important to note for future reference that the MFTF can also be modeled in the manner of Fig. 1b as a cross-correlation of $r(t)$ with a linear sum of time translates of $h(t)$,

$$\sum_{m=-N}^N a_m h(t - mT).$$

The decision-feedback equalizer (DFE) embodies a slightly different philosophy in which the DFE forward filter is allowed to respond to past (but not future) translates at $h(t)$; the residual interference from past data digits is then subtracted out prior to the decision threshold using past decisions. A realization of the DFE using again the MFTF approach is shown in Fig. 1d. The tap coefficients are now chosen to null the response to future data digits; this can be accomplished as $N \rightarrow \infty$.

The shortcoming of both the ZFE and DFE is that their linear filters remove intersymbol interference without regard to the effect on the noise; the result is that in eliminating the intersymbol interference (or a portion thereof) they necessarily enhance the noise.[†] It seems clear intuitively that since the DFE eliminates interference from only future data digits, it has more degrees of freedom than the ZFE and should therefore be capable of less noise enhancement. A proof that this is always the case has been given by Price;⁶ his method was to determine an explicit formula for the DFE S/N ratio using

[†] In addition, the DFE is susceptible to decision errors. The effect of errors will not receive consideration here.

Toeplitz form theory and compare it with the known S/N ratio of the ZFE.⁴ Additional interpretation of this result will be given in Section 3.1.

A review of some requisite material on linear spaces and MMSE linear estimation is given in Sections 2.1 and 2.2. Readers familiar with this material are nevertheless urged to scan these sections for notation to be employed in the remainder of the paper. The ZFE and DFE are reformulated in Section 2.3. In Section 2.4 the relationship between intersymbol interference and MMSE estimation is discussed, and a useful orthogonal expansion arising out of this relationship is derived in Section 2.5.

Section III develops a geometric theory of the ZFE and DFE. Conditions necessary and sufficient for the existence of these equalizers are given in Section 3.1, their performance is discussed in Section 3.2, a useful property of the DFE with regard to its output noise sequence is interpreted in Section 3.3, methods of calculating the tap-gains are derived in Section 3.4, and the relationship between finite and infinite transversal filter equalizers receives consideration in Section 3.5.

Sections II and III are concerned with additive white noise exclusively. Section IV extends the theory to colored Gaussian noise, nonstationary Gaussian noise, and a time-varying channel using the theory of reproducing kernel Hilbert spaces (RKHS).

II. AN EQUIVALENCE TO DISCRETE RANDOM PROCESSES

The structure of the intersymbol interference in (1) will now be shown to have an equivalence to a wide-sense stationary random process. The starting point will be a quick review of linear spaces and of linear mean-square error (MMSE) estimation of a random process.

2.1 Hilbert Space Notation¹⁰

An inner product space \mathcal{L} consists of a linear space together with a defined inner product $\langle x, y \rangle$ between two elements x and y . All spaces in this paper are Hilbert spaces, which consist of an inner product space satisfying an additional closure property (specifically, the limits of Cauchy sequences must be in the space). The inner product induces a norm, or "length" of a vector,

$$\|x\| \triangleq \langle x, x \rangle \quad (2)$$

and the notion of the distance between two vectors, $\|x - y\|$. The geometrical interpretation of these quantities is illustrated in Fig. 2.

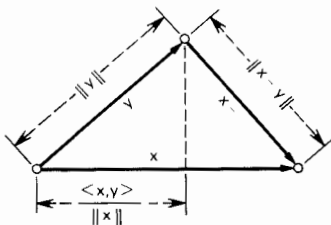


Fig. 2—Interpretation of inner product, norm, and distance.

A subspace of \mathcal{L} is any set of vectors which itself constitutes a linear space. If $x_k, k \in I$ is a countable or finite sequence of vectors, then we denote by $M(x_k, k \in I)$ the closure of the subspace consisting of all finite linear combinations of elements of the set $\{x_k, k \in I\}$ and call this the subspace spanned by the x_k 's. It is convenient to think of elements of $M(x_k, k \in I)$ as convergent (possibly) infinite sums of the form

$$\sum_{k \in I} a_k x_k$$

even though in some obscure cases not all elements can be expressed in this way.

In many minimization problems it is desired to find the element of some closed subspace M which is closest to a vector y ; the resulting element is called the projection of y on M , is denoted by $P(y; M)$, and satisfies the orthogonality property

$$\langle y - P(y; M), x \rangle = 0 \quad (3)$$

for all $x \in M$.[†] The geometric interpretation of (3) is shown in Fig. 3 for a one-dimensional subspace spanned by x ; for this case the projection must be a scalar times x and the validity of (3) is apparent.

2.2 Review of Linear Mean-Square Interpolation and Prediction^{2,3}

We will now quickly review the theory of linear mean-square estimation of a random variable.

The set of random variables with zero mean and finite variance is a linear space, since the sum of any two such random variables itself has these properties. This set is also a Hilbert space with inner product

$$\langle X, Y \rangle = E(XY), \quad (4)$$

[†] When, as in (3), a vector is orthogonal to every vector in M , it is said to be orthogonal to M .

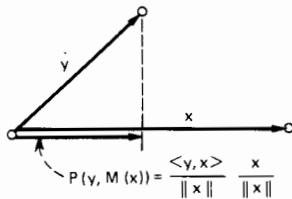


Fig. 3—Projection on subspace spanned by x .

where $E(\cdot)$ denotes expected value. It is standard to suppress the sample space dependence of a random variable as has been done in (4) because the geometric properties (inner product and norm) are determined by the value of the random variable on the whole sample space; that is, by its statistics in their entirety.

Consider now the following interpolation problem: Suppose that a sequence of zero-mean random variables X_k , $-\infty < k < \infty$, with finite variances are given and it is desired to estimate X_0 based on the observation of X_k , $k \neq 0$. If the estimate is further stipulated to be linear, it is the same as requiring that it be an element of $M(X_k, k \neq 0)$. Suppose that the estimate \hat{X}_0 is to be chosen in such a way that the mean-square error between X_0 and the estimate is minimized:

$$\min_{\hat{X}_0 \in M(X_k, k \neq 0)} E(X_0 - \hat{X}_0)^2. \quad (5)$$

From (4) and the previous section, the MMSE linear interpolator is

$$\hat{X}_0 = P[X_0, M(X_k, k \neq 0)], \quad (6)$$

the projection of X_0 on $M(X_k, k \neq 0)$.

A second estimation problem which will be of interest is the prediction of X_0 based only on X_k , $k > 0$ (an anticausal prediction). The MMSE linear predictor is the projection of X_0 on the subspace spanned by X_k , $k = 1, 2, \dots$, denoted by $P[X_0, M(X_k, k > 0)]$.

2.3 Zero-Forcing and Decision-Feedback Equalization

We are now prepared to restate the problem of determining the ZFE and DFE filters in a linear space context. It will be assumed that the basic pulse $h(t)$ in (1) has finite energy (i.e., is square integrable),

$$\int_{-\infty}^{\infty} h^2(t) dt < \infty. \quad (7)$$

The set of waveforms which satisfies (7) is a linear space, which we

denote by L_2 . L_2 is also a Hilbert space with inner product

$$\langle x, y \rangle = \int_{-\infty}^{\infty} x(t)y(t)dt \quad (8)$$

for any two L_2 waveforms $x(t)$ and $y(t)$. For the same reason that the sample space dependence of a random variable was suppressed in (4), the time dependence of the waveforms $x(t)$ and $y(t)$ has been suppressed on the left side of (8): it is the entire time waveform which determines the geometric properties.

The class of filters[†] which will be considered will be limited to those which can be modeled as an inner product (or cross-correlation) of the reception $r(t)$ with some L_2 waveform. A ZFE is a filter corresponding to a waveform $g_k(t)$ which does not respond to any translate of $h(t)$ except $h(t - kT)$,

$$\int_{-\infty}^{\infty} h(t - mT)g_k(t)dt = 0, \quad m \neq k, \quad (9)$$

but does respond to $h(t - kT)$,

$$\int_{-\infty}^{\infty} h(t - kT)g_k(t)dt \neq 0, \quad (10)$$

in order that there be a signal on which to base the decision. It is evident that if $g_0(t)$ satisfies (9) and (10) for $k = 0$, then they are also satisfied by $g_k(t) = g_0(t - kT)$ for $k \neq 0$. Written in inner product notation, (9) and (10) become

$$\langle h_k, g_0 \rangle = 0, \quad k \neq 0, \quad (11)$$

$$\langle h_0, g_0 \rangle \neq 0, \quad (12)$$

where we have written h_k for $h(t - kT)$. The analogous condition for a DFE forward filter is

$$\langle h_k, g_0 \rangle = 0, \quad k > 0, \quad (13)$$

$$\langle h_0, g_0 \rangle \neq 0. \quad (14)$$

The forms of the ZFE and DFE in this symbolic notation are shown in Figs. 4a and b. The output of the linear filter is a function of B_k (a single data digit) for a ZFE and B_{k-m} , $m > 0$ (all past data digits) for a DFE. The tap-gains of the feedback transversal filter storing past decisions for the DFE are equal to the responses of g_0 to previous pulses, $\langle g_0, h_{-m} \rangle$, $m > 1$.

[†] In the case of the DFE, we refer only to the forward filter.

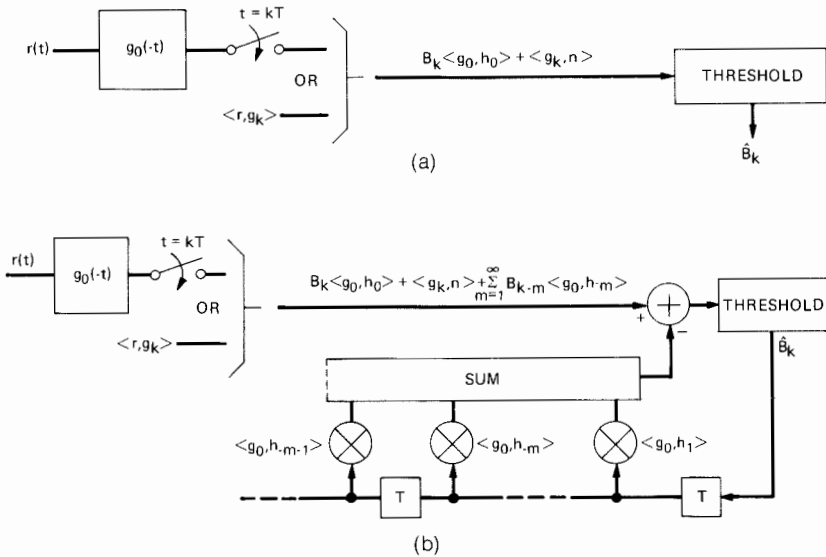


Fig. 4—Symbolic representations of the two equalizers: (a) zero-forcing equalizer; (b) decision-feedback equalizer.

2.4 A Congruence Relationship

Two Hilbert spaces which display an identical geometrical structure are said to be congruent¹¹ or unitarily equivalent.¹⁰ Specifically, in order for two Hilbert spaces to be congruent, there must exist between them a one-to-one and onto linear mapping which preserves norms and inner products. Although the elements of two such spaces may be quite different entities, when considered as elements of their respective Hilbert spaces they have the same geometrical structure.

Define the autocorrelation function of the pulse sequence,

$$R_k = \langle h_m, h_{m+k} \rangle. \tag{15}$$

It follows from the inequality

$$0 \leq \left\| \sum_{m=0}^N \alpha_m h_{k_m} \right\|^2 = \sum_{m=0}^N \sum_{n=0}^N \alpha_m \alpha_n R_{k_m - k_n}$$

that $\{R_k\}$ is a nonnegative definite function. Therefore, there exists a second-order discrete random process $\{X_k\}$ which has autocorrelation R_k ,

$$\begin{aligned} \langle X_m, X_{m+k} \rangle &= E(X_m, X_{m+k}) \\ &= R_k. \end{aligned} \tag{16}$$

For the random process defined in (16), $M(h_k, k \in I)$ and $M(X_k, k \in I)$ are congruent through the obvious mapping

$$\phi \left[\sum_{m=1}^N \alpha_m h_{k_m} \right] = \sum_{m=1}^N \alpha_m X_{k_m} \quad (17)$$

which is a unitary linear transformation. To verify this, observe that the mapping is linear, preserves norms,

$$\begin{aligned} \left\| \phi \left(\sum_{m=1}^N \alpha_m h_{k_m} \right) \right\|^2 &= \left\| \sum_{m=1}^N \alpha_m X_{k_m} \right\|^2 \\ &= \sum_{m=1}^N \sum_{n=1}^N \alpha_m \alpha_n R_{k_m - k_n} \\ &= \left\| \sum_{m=1}^N \alpha_m h_{k_m} \right\|^2, \end{aligned} \quad (18)$$

and preserves inner products by an equally simple derivation.

The mapping of (17) is only defined for finite sums. When I is an infinite set, ϕ can be extended to all of $M(h_k, k \in I)$ by taking limits in the mean. For any $f \in M(h_k, k \in I)$ there exists a sequence $\{f_k\}$, each consisting of a finite sum of the form of (17), such that $f_k \rightarrow f$. Since $\phi(f_k)$ is a Cauchy sequence from (18), we define $\phi(f)$ as the limit of $\phi(f_k)$, which is in $M(X_k, k \in I)$ by completeness.

There is an additional congruence which is useful. From the definition of R_k in (15), we see that

$$\begin{aligned} R_k &= \frac{1}{2\pi} \int_{-\infty}^{\infty} |H(\omega)|^2 e^{j\omega k T} d\omega \\ &= \frac{1}{2\pi} \int_{-\pi/T}^{\pi/T} R(\omega) e^{j\omega k T} d\omega, \end{aligned} \quad (19)$$

where

$$\begin{aligned} R(\omega) &\triangleq \sum_{m=-\infty}^{\infty} \left| H \left(\omega + m \frac{2\pi}{T} \right) \right|^2 \\ &= T \sum_{n=-\infty}^{\infty} R_n e^{jn\omega T}, \end{aligned} \quad (20)$$

where $R(\omega)$ is an equivalent power spectrum of the channel. From (16), $R(\omega)/T$ is the power spectrum of the random process $\{X_k\}$. Let $L_2(-\pi/T, \pi/T; R)$ denote the Hilbert space of all complex-valued Lebesgue measurable functions $f(\omega)$ with domain $|\omega| < \pi/T$ which satisfy

$$\|f(\omega)\|^2 = \frac{1}{2\pi} \int_{-\pi/T}^{\pi/T} |f(\omega)|^2 R(\omega) d\omega < \infty \quad (21)$$

with the obvious definition of the inner product. A frequently invoked congruence is between $M(X_k, -\infty < k < \infty)$ and $L_2(-\pi/T, \pi/T; R)$.² By implication, $L_2(-\pi/T, \pi/T; R)$ and $M(h_k, -\infty < k < \infty)$ are also congruent through the mapping

$$\psi \left(\sum_{m=1}^N \alpha_m h_{k_m} \right) = \sum_{m=1}^N \alpha_m e^{-j\omega k_m T} \tag{22}$$

as is readily verified.

In the remainder of this paper, the congruence demonstrated in this section will be exploited to demonstrate that many available results on MMSE interpolation and prediction theory are directly applicable to the equalization problems posed in Section 2.3.

2.5 An Orthogonal Expansion

The congruence relation of Section 2.4 will be used in this section to establish an orthogonal expansion in $M(h_k, -\infty < k < \infty)$ which will be particularly useful in the sequel.

Define the element

$$e_k^+ \triangleq h_k - P[h_k, M(h_m, m > k)] \tag{23}$$

which is the difference between a translate of $h(t)$, h_k , and its projection on the subspace of translates to its right. It will be shown later that this element is of particular significance to the DFE. For the moment, however, note that e_k^+ is equivalent to the MMSE prediction error of X_k based on $X_m, m > k$, since the projection is the optimum linear predictor. It is well known³ that the successive prediction errors of a random process are uncorrelated random variables. The equivalent statement relating to e_k^+ is that

$$\langle e_m^+, e_n^+ \rangle = \|e_0^+\|^2 \delta_{m,n} \tag{24}$$

and it is an orthogonal sequence.[†] This is readily demonstrated directly by noting that e_m^+ is orthogonal to $M(h_k, k \geq m)$, which contains e_n^+ for $n > m$. Hence, (24) follows for $n > m$ and by symmetry for $n < m$ also.

From (24) it follows that as long as

$$\|e_0^+\| > 0 \tag{25}$$

the sequence

$$w_n \triangleq e_n^+ / \|e_0^+\|, \quad -\infty < n < \infty, \tag{26}$$

is an orthonormal set in L_2 . The significance of (25) is that the equiv-

[†] The norm of e_k^+ is independent of k since e_k^+ is a time translate of e_0^+ .

alent random process must not be linearly predictable with vanishing mean-square error (in the language of Ref. 3, p. 564, X_k must be "regular," or "nondeterministic").

Expanding h_n in a Fourier series in w_n ,

$$\begin{aligned} h_n &= u_n + v_n \\ u_n &= \sum_{m=-\infty}^{\infty} c_m w_{n+m} \\ c_m &\triangleq \langle w_{n+m}, h_n \rangle = \langle w_m, h_0 \rangle \\ \langle v_n, w_m \rangle &= 0, \quad -\infty < n < \infty, \quad -\infty < m < \infty, \end{aligned} \quad (27)$$

where v_n is the remainder. Equation (27) can be simplified by observing that

$$\langle w_m, h_0 \rangle = 0, \quad m < 0,$$

since $h_0 \in M(h_k, k \geq 0)$ and w_m is orthogonal to $M(h_k, k \geq m+1)$, which contains $M(h_k, k \geq 0)$ when $m < 0$. In addition, it can be shown (Ref. 3, pp. 571-575) that $v_n = 0$, since the spectrum under consideration here is absolutely continuous.[†] Thus, (27) reduces to

$$\begin{aligned} h_n &= \sum_{m=0}^{\infty} c_m w_{n+m} \\ c_m &= \langle h_0, w_m \rangle. \end{aligned} \quad (28)$$

The expansion of (28), which is used in the theory of linear prediction,^{2,3} is similar in spirit to a straightforward Gram-Schmidt orthogonalization process, but is much more useful in that the coefficients of the expansion are independent of n . The main shortcoming of the expansion (28) is requirement (25).

The formula for c_m given in (27) is not very useful in explicitly evaluating the coefficients of (28). A more useful method of evaluation is to observe that it is a spectral factorization problem. Defining the bilateral z -transform[‡] of the autocorrelation,

$$R^*(z) = \sum_{m=-\infty}^{\infty} R_m Z^m, \quad (29)$$

we claim that

$$R^*(z) = \sum_{n=0}^{\infty} c_n Z^n \sum_{n=0}^{\infty} c_n Z^{-n}, \quad (30)$$

[†] This is by virtue of the fact that integral (21) is in terms of $R(\omega)d\omega$; i.e., the underlying measure is presumed to be absolutely continuous with respect to Lebesgue measure.

[‡] Note that we define the z -transform in positive powers of z .

where the c_m are given by (28). To show (30), first calculate R_j from (15),

$$\begin{aligned}
 R_j &= \langle h_0, h_j \rangle \\
 &= \sum_{m=0}^{\infty} \sum_{n=0}^{\infty} c_m c_n \langle w_m, w_{j+n} \rangle \\
 &= \begin{cases} \sum_{n=0}^{\infty} c_n c_{n+j}, & j \geq 0 \\ \sum_{n=-j}^{\infty} c_n c_{n+j}, & j < 0. \end{cases} \tag{31}
 \end{aligned}$$

Similarly, the right side of (30) can be manipulated,

$$\sum_{n=0}^{\infty} \sum_{m=0}^{\infty} c_n c_m Z^{n-m} = \sum_{m=0}^{\infty} \sum_{n=0}^{\infty} c_n c_{n+m} Z^m + \sum_{m=1}^{\infty} \sum_{n=-m}^{\infty} c_n c_{n-m} Z^{-m}, \tag{32}$$

and comparing (31) and (32), (30) is established. The representation of (30) is not unique. However, Doob (Ref. 3, p. 160) shows that the coefficients of (27) uniquely satisfy (30) when the additional conditions

$$\sum_{n=0}^{\infty} c_n Z^n \neq 0, \quad |Z| < 1, \tag{33}$$

$$\sum_{n=0}^{\infty} c_n^2 < \infty \tag{34}$$

are required.[†] The necessity of (34) is obvious from (27), while the reason why (33) is needed is that otherwise (30) could be satisfied on the unit circle by another sequence with a larger zeroth term, contradicting the fact that

$$c_0 = \|e_0^+\|. \tag{35}$$

Equation (35) follows from the observation that $M(h_k, k \geq n) = M(w_k, k \geq n)$ and therefore $P[h_n, M(h_k, k \geq n + 1)] = \sum_{m=1}^{\infty} c_m w_{n+m}$ or

$$e_n^+ = c_0 w_n. \tag{36}$$

A simple example will serve to illustrate (30). Suppose $h(t)$ has an exponential autocorrelation with

$$R_k = A^{|k|}, \quad 0 < A < 1. \tag{37}$$

[†] Of course, condition (25) is also required.

Direct calculation of (29) reveals that

$$R^*(z) = \frac{1 - A^2}{(1 - AZ)(1 - A/Z)} \tag{38}$$

which is in the form of (30) with

$$c_n = \sqrt{1 - A^2} A^n. \tag{39}$$

The validity of (39) can be demonstrated directly for this simple example by noting that

$$e_k^+ = h_k - Ah_{k+1} \tag{40}$$

(as can be verified by showing that e_k^+ is orthogonal to h_m , $m \geq k + 1$) and thus

$$\begin{aligned} w_n &= \frac{h_n - Ah_{n+1}}{\|h_n - Ah_{n+1}\|} \\ &= \frac{h_n - Ah_{n+1}}{\sqrt{1 - A^2}}. \end{aligned} \tag{41}$$

From (28),

$$\begin{aligned} c_m &= \langle h_0, w_m \rangle \\ &= \sqrt{1 - A^2} A^m \end{aligned} \tag{42}$$

agreeing with (39).

The procedure for higher-order rational spectra is equally simple. From (29) and the fact that R_m is real and even ($R_{-m} = R_m$), it follows that

$$R^*(z) = R^*\left(\frac{1}{z}\right). \tag{43}$$

Thus, for every zero a_i and pole b_i of $R^*(z)$, a_i^{-1} and b_i^{-1} are also a zero and a pole respectively. Thus, $R^*(z)$ can be written in the form

$$R^*(z) = K \frac{\prod_{i=1}^m (1 - a_i z) \left(1 - \frac{a_i}{z}\right)}{\prod_{i=1}^n (1 - b_i z) \left(1 - \frac{b_i}{z}\right)} \tag{44}$$

$$|a_i|, \quad |b_i| < 1$$

so that from (30)

$$C(z) = \sum_{n=0}^{\infty} c_n Z^n = \sqrt{K} \frac{\sum_{i=1}^m (1 - a_i z)}{\sum_{i=1}^n (1 - b_i z)}, \tag{45}$$

where (33) has been insured by the choice of zeros in (45).

When $R^*(z)$ is not rational, a more general method of determining the coefficients of (28) is required. For this purpose, we use the equivalent power spectrum of (20). The first form in (20) is the one required for analytically determining $C(z)$, whereas the second form is the one which would usually be used in numerical calculations. The relationship of $R(\omega)$ to $R^*(z)$ is, of course,

$$R(\omega) = TR^*(e^{j\omega T}), \tag{46}$$

the evaluation of $R^*(z)$ on the unit circle. The equivalent of (30) for $R(\omega)$ is

$$\frac{R(\omega)}{T} = \left| \sum_{k=0}^{\infty} c_k e^{j\omega k T} \right|^2. \tag{47}$$

Intuitively, (47) requires the expansion of $\sqrt{R(\omega)/T}$, with an arbitrary phase characteristic, in a complex Fourier series with only positive frequencies. Following Doob (Ref. 3, p. 161), expand $\log \sqrt{R(\omega)/T}$ in a Fourier series,

$$\frac{1}{2} \log \frac{R(\omega)}{T} = \sum_k r_k e^{j\omega k T}. \tag{48}$$

This is always possible because, as will be demonstrated later, in order for (25) to be satisfied, it is necessary and sufficient that $\log R(\omega)$ be integrable. Define

$$g(z) = r_0 + 2 \sum_{k=1}^{\infty} r_k z^k \tag{49}$$

and note that

$$\text{Re } g(e^{j\omega T}) = \frac{1}{2} \log \frac{R(\omega)}{T}. \tag{50}$$

We claim that

$$C(z) = e^{g(z)} \tag{51}$$

satisfies (47), since

$$|C(e^{j\omega T})| = \exp[\text{Re } g(e^{j\omega T})] = \sqrt{\frac{R(\omega)}{T}}.$$

Equation (33) is also satisfied since $g(z)$ is analytic for $|z| < 1$.

Equation (51) is an analytic solution to the problem initially posed, but a practical means of applying it numerically is required. It is shown in Appendix A that the Fourier coefficients of (48) can be calculated efficiently and accurately using the fast Fourier transform (FFT) algorithm. The second difficulty is in determining $C(z)$ from

$g(z)$ in (51). This is easily resolved by noting that

$$\begin{aligned} c_m &= \frac{1}{m!} \left. \frac{d^m}{dz^m} C(z) \right|_{z=0} & m \geq 0 \\ r_m &= \frac{1}{2m!} \left. \frac{d^m}{dz^m} g(z) \right|_{z=0} & m \geq 1 \\ c_0 &= e^{r_0} \end{aligned} \quad (52)$$

and applying Leibniz's differentiation rule

$$\frac{d^n}{dz^n} uv = \sum_{m=0}^n \binom{n}{m} \frac{d^{n-m}u}{dz^{n-m}} \frac{d^m v}{dz^m}$$

to the product

$$\begin{aligned} \frac{d^n}{dz^n} C(z) &= \frac{d^{n-1}}{dz^{n-1}} \left(e^{g(z)} \frac{dg(z)}{dz} \right) \\ &= \sum_{m=0}^{n-1} \binom{n-1}{m} \frac{d^{n-m}g(z)}{dz^{n-m}} \frac{d^m C(z)}{dz^m} \end{aligned}$$

and, setting $z = 0$,

$$c_n = \frac{2}{n} \sum_{m=0}^{n-1} (n-m)r_{n-m}c_m, \quad n \geq 1. \quad (53)$$

Equations (52)–(53) give us a practical recursive method of determining the coefficients of (28) when the channel spectrum is not rational.

III. GEOMETRIC THEORY OF THE ZERO-FORCING AND DECISION-FEEDBACK EQUALIZERS

The zero-forcing equalizer (ZFE) and decision-feedback equalizer (DFE) have been introduced in Sections 1.1 and 2.3. In this section, we will describe fully the characteristics of these equalizers in the context of the geometric structure developed in Section II.

3.1 Conditions for the Existence of the ZFE and DFE

The existence of a ZFE and DFE will now be related to the interpolation and prediction of the equivalent random process defined in Section 2.2. This relationship will then be used to obtain directly the known conditions for their existence.

The first observation is that the subspaces $M(h_k, k \neq 0)$ and $M(X_k, k \neq 0)$ are identical, as are the subspaces $M(h_k, k > 0)$ and $M(X_k, k > 0)$. The element

$$e_0 = h_0 - P[h_0, M(h_k, k \neq 0)] \quad (54)$$

is the same as the interpolation error vector defined in Section 2.2, $(X_0 - \hat{X}_0)$, while the prediction error vector is the same as

$$e_0^+ = h_0 - P[h_0, M(h_k, k > 0)]. \quad (55)$$

These two vectors are likely candidates for a ZFE and a DFE because they are orthogonal to the subspaces $M(h_k, k \neq 0)$ and $M(h_k, k > 0)$ respectively [see Section 2.1 and eq. (3)]. Hence, they satisfy (11) and (13) respectively. To verify that they are indeed a ZFE and a DFE, conditions (12) and (14) must be checked. Noting that e_0 is orthogonal to $M(h_k, k \neq 0)$, we have

$$\begin{aligned} \langle e_0, h_0 \rangle &= \langle e_0, h_0 - P[h_0, M(h_k, k \neq 0)] \rangle \\ &= \|e_0\|^2 \end{aligned} \quad (56)$$

by definition (54). Similarly, it follows that

$$\langle e_0^+, h_0 \rangle = \|e_0^+\|^2. \quad (57)$$

Thus, we see that a necessary and sufficient condition for e_0 (e_0^+) to be a ZFE (DFE) is that $\|e_0\| > 0$ ($\|e_0^+\| > 0$). By definition, the projection of h_0 on a subspace is the element of that subspace which is at a minimum distance from h_0 , and hence $\|e_0\|$ and $\|e_0^+\|$ are the minimum distances between h_0 and $M(h_k, k \neq 0)$ and $M(h_k, k > 0)$ respectively. Since $\|e_0\|$ can only vanish if $h_0 \in M(h_k, k \neq 0)$, and similarly for $\|e_0^+\|$, it follows that e_0 (e_0^+) is a ZFE (DFE) if and only if $h_0 \notin M(h_k, k \neq 0)$ [$h_0 \notin M(h_k, k > 0)$]. Physically, these conditions mean that $h(t)$ must not be representable as an infinite weighted sum of a subset of its own translates. Geometrically, it is evident in Fig. 5 that, as long as $\|e_0\| > 0$ (or $\|e_0^+\| > 0$), e_0 (or e_0^+) will have a component in the direction of h_0 and the equalizer will have a response to the desired signal.

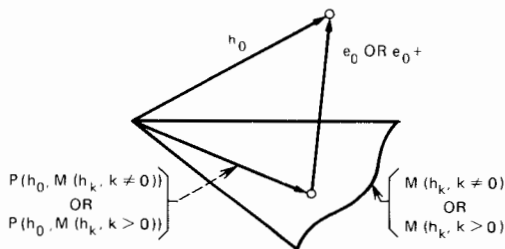


Fig. 5—Geometric interpretation of the zero-forcing equalizer and decision-feedback equalizer.

The weighting functions (54)–(55) can, under reasonable conditions,[†] be written in the form of a convergent linear sum of translates of h_0 ,

$$e_0 = h_0 - \sum_{k \neq 0} a_k h_k \quad (58)$$

$$e_0^+ = h_0 - \sum_{k > 0} a_k^+ h_k \quad (59)$$

for some coefficients a_k^+ . This demonstrates that these two elements are just the matched filter followed by transversal filter (MFTF) discussed in Section 1.1. It will be shown in the next section that the MFTF has particular significance, in that it maximizes the S/N ratio.

In general, there will be many ZFE's and DFE's other than (58)–(59). An example of a different ZFE is the element

$$h'_0 - P[h'_0, M(h_k, k \geq 0)]$$

for any h'_0 such that

$$\begin{aligned} \langle h'_0, h_0 \rangle &\neq 0 \\ h'_0 &\notin M(h_k, k \neq 0). \end{aligned}$$

An interesting question that arises is, then, whether there ever exists a ZFE and DFE when their corresponding MFTF's do not exist. To see that the answer is no for the ZFE (the proof for the DFE is identical), note that if $h_0 \in M(h_k, k \neq 0)$, then any g_0 orthogonal to $M(h_k, k \neq 0)$ is also necessarily orthogonal to h_0 .[‡] Thus, we have proven the following theorem:

Theorem 1: The following five statements are equivalent:

1. $h_0 \notin M(h_k, k \neq 0)$ [$h_0 \notin M(h_k, k > 0)$].
2. $\|e_0\| > 0$ [$\|e_0^+\| > 0$].
3. There exists a ZFE [DFE].
4. There exists a ZFE [DFE] of the form of eq. (54) [eq. (55)], the MFTF.
5. The random process defined in (16) cannot be linearly interpolated [predicted] with vanishing mean-square error.

The fifth condition of Theorem 1 follows from our earlier identification of e_0 and e_0^+ as the interpolation and prediction errors, respectively, of the equivalent random process. This observation also enables us to pull from the literature formulas for the norms of e_0 and e_0^+ . The follow-

[†] This will be discussed fully in Section 3.5.

[‡] We also make use of the trivial observation that any g_0 satisfying (11) is orthogonal to $M(h_k, k \neq 0)$.

ing corollary follows directly from the known formulas for the interpolation and prediction errors of a random process,^{2,3}

$$\|e_0\|^2 = \left[\frac{T^2}{2\pi} \int_{-\pi/T}^{\pi/T} R^{-1}(\omega) d\omega \right]^{-1} \quad (60)$$

$$\|e_0^+\|^2 = \frac{1}{T} \exp \left[\frac{T}{2\pi} \int_{-\pi/T}^{\pi/T} \log R(\omega) d\omega \right]. \quad (61)$$

Corollary 1: A ZFE [DFE] exists if and only if $R^{-1}(\omega)$ [$\log R(\omega)$] is integrable.

Both conditions relate to the fashion in which $R(\omega)$ vanishes. In particular, both require that $R(\omega)$ vanish on at most a set of measure zero. The relationship of (60) and (61) will be discussed more fully in the sequel.

It should be noted also that (61) follows directly from the orthogonal expansion of Section 2.5. From (35) we know that $\|e_0^+\|^2$ equals c_0^2 , while (52) gives a relation for c_0 . When the Fourier series of (48) is inverted and r_0 is substituted into (52), (61) results.

3.2 Performance of the Equalizers

It will now be shown that the MFTF among all ZFE's and DFE's maximizes the S/N ratio and minimizes the error probability in white Gaussian noise. The derivation will be a simple application of the Schwarz inequality.

Assume that the additive noise in (1) is white and Gaussian. Then the decision axis which is applied to a threshold is, for the ZFE,

$$\langle g_0, r \rangle = B_0 \langle g_0, h_0 \rangle + \langle g_0, n \rangle, \quad (62)$$

where $\langle g_0, n \rangle = n_0$ is a Gaussian random variable with mean zero and variance

$$E n_0^2 = \frac{N_0}{2} \|g_0\|^2 \quad (63)$$

and $N_0/2$ is the two-sided spectral density of the noise. The minimum probability of error decision strategy is then to apply $\langle g_0, r \rangle$ to a series of $M - 1$ thresholds, with the specific thresholds depending on the probability law on B_k . For any such law and series of thresholds the probability of error will be a monotone decreasing function of the S/N ratio, which is proportional to

$$S/N \propto \frac{\langle g_0, h_0 \rangle^2}{\|g_0\|^2}, \quad (64)$$

since $\langle g_0, n \rangle$ is a zero-mean Gaussian random variable with variance proportional to $\|g_0\|^2$. Noting from (11) that g_0 is orthogonal to $P[h_0, M(h_k, k \neq 0)]$ whenever g_0 is a ZFE, (64) can be rewritten

$$S/N \propto \frac{\langle g_0, e_0 \rangle^2}{\|g_0\|^2} \leq \|e_0\|^2 \quad (65)$$

by the Schwarz inequality, with equality if and only if g_0 equals e_0 (the MFTF) within a multiplicative constant. Thus, the MFTF, among all ZFE's, maximizes the S/N ratio. By the same method an identical result can be demonstrated for the DFE, if it is assumed that the decision-feedback mechanism correctly cancels the tails of earlier pulses.

The preceding derivation, which is a generalization of the Schwarz inequality derivation of the matched filter, has the geometric interpretation of Fig. 6. In writing (65), the maximization of (64) is restricted to those g_0 which lie in the hyperplane orthogonal to $P[h_0, M(h_k, k \neq 0)]$. Since every ZFE is also orthogonal to this vector, it follows that the hyperplane so described contains the set of all ZFE's. However, the maximization over elements of the hyperplane does not guarantee a result which is a ZFE. The vector in the hyperplane which has the greatest component in the direction of h_0 per unit length is evidently the one which lines up with e_0 , as verified by (65). Fortunately, this vector also turns out to be a ZFE, so that the maximization is complete.

An additional observation relative to (65) is that the maximum S/N ratio is proportional to $\|e_0\|^2$ for the ZFE and $\|e_0^+\|^2$ for the DFE. The maximum S/N ratio is therefore directly proportional to the mean-square interpolation and prediction errors of the equivalent random process. Thus, the maximum S/N ratios of the ZFE and DFE are given by (60) and (61) respectively, while the factor by which the

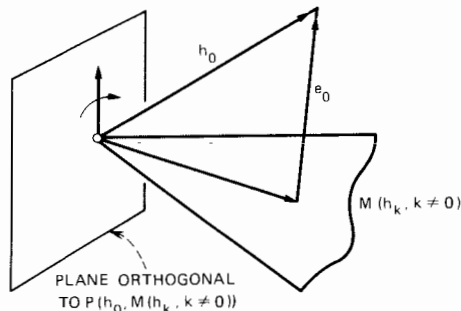


Fig. 6—S/N ratio maximized by the MFTF.

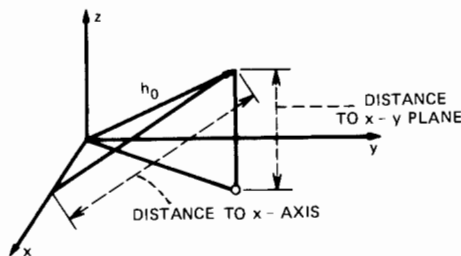


Fig. 7—Geometric interpretation of eq. (66).

S/N ratio is reduced relative to an isolated pulse with matched filter detection is obtained by dividing by R_0 , the isolated pulse energy.

Price⁶ derived (61) by a different method and used the geometric mean inequality for integrals to show from (60) and (61) that

$$\|e_0\|^2 \leq \|e_0^+\|^2. \quad (66)$$

This important result implies that (i) the S/N ratio of the DFE MFTF always exceeds that of the ZFE MFTF,[†] and (ii) a DFE exists whenever a ZFE exists [the contrary is not true, as demonstrated by the important example of algebraic zeros in $R(\omega)$ ⁶]. Using the geometric method we have developed, two interpretations of (66) can be given. First, it is intuitively apparent that the mean-square interpolation error of a random process will be smaller than the mean-square prediction error, because an interpolation is based on more information; similarly, there will be some processes for which interpolation, but not prediction, with zero mean-square error is possible. Second, since $M(h_k, k \neq 0)$ contains $M(h_k, k > 0)$, the distance between h_0 and $M(h_k, k \neq 0)$ (equal to $\|e_0\|^2$) must be smaller than the distance between h_0 and $M(h_k, k > 0)$ (equal to $\|e_0^+\|^2$). This second interpretation is a rigorous way of establishing (66) by a method more direct than the integral inequality. It has the geometric interpretation of Fig. 7, where the distance between a vector h_0 and the larger subspace (the x - y plane) is less than between h_0 and the subspace it contains (the x axis).

The performance of the ZFE and DFE can be evaluated for any particular channel spectrum using (60)–(61). In particular, (60)–(61) can be evaluated in closed form for rational spectra. A different approach, which allows us to evaluate the tap-gains of the equalizers as well, will be pursued in Section 3.4.

[†] This result neglects the effect of decision errors on the DFE.

3.3 On the DFE White Output Noise Property

As observed by Price,⁶ the DFE forward filter is identical to the "whitened matched filter" employed by Forney¹² as the first element of his maximum likelihood detector. The property of this filter which is essential to Forney's application is that the noise sequence at the filter output is uncorrelated. As with the other properties of this filter, this one has a simple explanation in terms of the relationship to linear prediction.

Identifying e_k^+ as $e_0^+(t - kT)$, the noise sequence at the DFE forward filter output is $\langle e_k^+, n \rangle$. Since $n(t)$ is white noise, this sequence will be uncorrelated if and only if

$$\langle e_m^+, e_n^+ \rangle = 0, \quad m \neq n. \quad (67)$$

The validity of (67) and an interpretation of this result in terms of the uncorrelated nature of the successive prediction errors of a random process has already been given in Section 2.5.

3.4 Determination of Tap-Gains

In this section, we will use the orthogonal expansion of Section 2.5 to derive methods of determining the tap-gains of the forward and feedback filters of the MFTF DFE. For comparison purposes the well-known relation for the tap-gains of the ZFE will also be briefly developed.

If we write the weighting response of the MFTF ZFE as

$$a_0 e_0 = \sum_{k=-\infty}^{\infty} a_k h_k, \quad (68)$$

where the tap-gains of the transversal filter are a_k , $-\infty < k < \infty$, condition (11)-(12) becomes

$$\begin{aligned} \langle e_0, h_m \rangle &= \|e_0\|^2 \delta_{m,0} \\ &= \frac{1}{a_0} \sum_k a_k R_{m-k}. \end{aligned} \quad (69)$$

Taking the bilateral z -transform of (69),

$$a_0 \|e_0\|^2 = A(z) R^*(z), \quad (70)$$

where $A(z)$ is the z -transform of the tap-gains

$$A(z) \triangleq \sum_k a_k z^k. \quad (71)$$

Thus, from (70),

$$A(z) = \frac{a_0 \|r_0\|^2}{R^*(z)}. \quad (72)$$

This filter is illustrated in Fig. 8a. When $h(t)$ is applied to the input of a matched filter and the output sampled at a rate of $1/T$, the output has z -transform $R^*(z)$. The transversal filter weighting response has a z -transform proportional to $R^*(z)^{-1}$, so that the output is consistent with (69).

The S/N ratio of the ZFE, given by (60), is readily derived from (72). Writing the relation for tap-gain zero,

$$a_0 = \frac{1}{2\pi j} \oint \frac{A(z)}{z} dz = \frac{a_0 \|e_0\|^2}{2\pi j} \oint \frac{dz}{zR^*(z)}, \quad (73)$$

and solving for $\|e_0\|^2$, we immediately get (60) using (46).

As an example, for the exponential autocorrelation of (37), (72) becomes

$$A(z) = a_0 \|e_0\|^2 \left[-\frac{A}{1-A^2} z^{-1} + \frac{1+A^2}{1-A^2} - \frac{A}{1-A^2} z \right] \quad (74)$$

from which we get

$$\begin{aligned} \|e_0\|^2 &= \frac{1-A^2}{1+A^2} \\ a_{-1} &= a_1 = -\frac{a_0 A}{1+A^2} \\ a_k &= 0, \quad |k| > 1, \end{aligned} \quad (75)$$

a result derived by Tufts¹³ by another method. This example points out that it is not ever necessary to actually evaluate (60) when the channel spectrum is rational, but rather the performance can be obtained by equating the zero-order tap-gains of (72) in the manner of (73).

The situation with the DFE is only slightly more complicated. In this case the DFE filter is

$$a_0^+ e_0^+ = \sum_{k=0}^{\infty} a_k h_k, \quad (76)$$

where only taps on one side are involved. Substituting from (28) and (36),

$$\begin{aligned} a_0^+ c_0 w_0 &= \sum_{k=0}^{\infty} a_k^+ \sum_{m=0}^{\infty} c_m w_{k+m} \\ &= \sum_{m=0}^{\infty} w_m \sum_{k=0}^m a_k^+ c_{m-k}, \end{aligned} \quad (77)$$

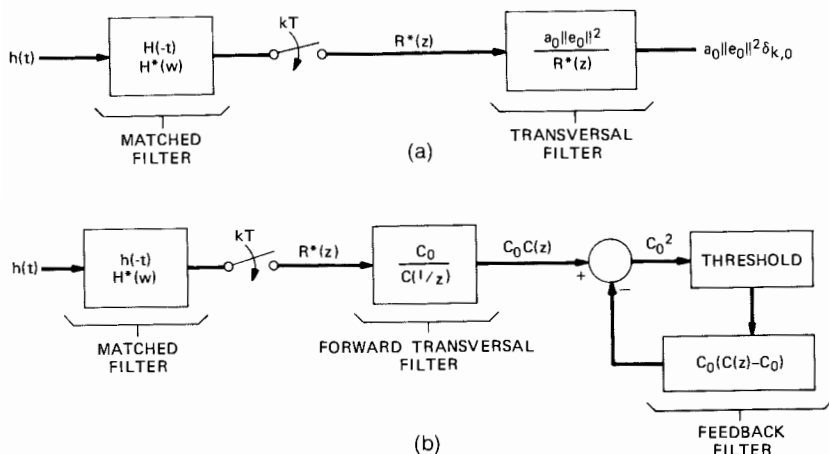


Fig. 8—Spectral representations of the MFTF zero-forcing equalizer (a) and decision-feedback equalizer (b).

and equating coefficients,

$$\sum_{k=0}^m a_k^+ c_{m-k} = \begin{cases} a_0^+ c_0, & m = 0 \\ 0, & m > 0. \end{cases} \quad (78)$$

From (78) we get a recursion relation for the tap coefficients which is useful for nonrational spectra,

$$a_m^+ = -\frac{1}{c_0} \sum_{k=0}^{m-1} a_k^+ c_{m-k}, \quad (79)$$

and a z -transform relation which is useful for rational spectra,

$$A^+(z) = \frac{a_0^+ c_0}{C(z)}, \quad (80)$$

where $A^+(z)$ is the z -transform of the tap-gains of (76). Performing (80) again for the autocorrelation of (37),

$$\begin{aligned} A^+(z) &= a_0^+ (1 - Az) \\ \|e_0^+\|^2 &= c_0^2 = 1 - A^2 \end{aligned} \quad (81)$$

which is consistent with (40) and is larger than $\|e_0\|^2$ by a factor of $(1 + A^2)$. As with the ZFE, the performance of the DFE can be determined for rational spectra without the explicit evaluation of (61).

The comparison of (80) with (72) is interesting, in that they are identical except for the fact that in (80) $C(z)$ is substituted for $R^*(z)$

in (72). The annulus of convergence of $A(z)$ will always include the unit circle, since $R^*(z)$ converges in an annulus containing the unit circle. Similarly, $C(z)$ is analytic and nonzero in a region containing the unit disk, and hence $A^+(z)$ will have only positive powers of z and converge in a region containing the unit disk. Note that these properties of $A^+(z)$ are critically dependent on (33) being satisfied.

The spectral factorization method of determining the tap-gains of the DFE was given by Monsen⁵ for rational spectra. Price⁶ gave a formula valid for arbitrary spectra, but it is difficult to evaluate numerically. Since (79) is valid for arbitrary spectra, the method presented here represents a synthesis of the appeal and computational simplicity of the spectra factorization method with the generality of Price's Toeplitz form result.

We also need the tap-gains of the feedback filter for the DFE. From Fig. 4, the required feedback tap-gains are given by $\langle e_0^+, h_{-n} \rangle$, $1 \leq n < \infty$. From (36) and (28),

$$\begin{aligned} b_n &= \langle e_0^+, h_{-n} \rangle = c_0 \sum_{m=0}^{\infty} c_m \langle w_0, w_{m-n} \rangle \\ &= c_0 c_n. \end{aligned} \quad (82)$$

Thus, the frequency response of the feedback filter is given by

$$\sum_{m=1}^{\infty} b_m z^m = c_0 [C(z) - c_0]. \quad (83)$$

The z -transform representation of the DFE just derived is illustrated in Fig. 8b. When an isolated pulse $h(t)$ is applied to the matched filter, the sampled output has z -transform $R^*(z)$. The transversal filter multiplies by $A^+(1/z) = c_0/C(1/z)$, as can be verified from (76).[†] The z -transform of the forward transversal filter output is $c_0 C(z)$ because of (30), which verifies the causal response which is characteristic of the DFE. The output of the feedback filter of (83) is then subtracted, to yield (hopefully) a delta function response c_0^2 . The reader can verify that when the threshold is replaced by a gain of $1/c_0^2$ (the noise-free case) the response is as represented.

3.5 Finite Transversal Filter Equalizers

The previous sections have considered the rather idealized case of infinite transversal filter equalizers. Since only finite equalizers can

[†] This is because (76) is not in the form of a convolution sum. This distinction was not relevant to the ZFE due to the symmetry of that filter.

actually be implemented, the important question arises as to when and in what sense the infinite equalizer can be approximated by a finite one.

We have already seen in the example of the exponential autocorrelation that the infinite equalizer can degenerate into a finite transversal filter for some channel spectra. This will happen whenever $A(z)$ and $A^+(z)$ are finite polynomials in z . From (72) and (80) we see that this will occur whenever $R^*(z)$ is a rational function which has no zeros (only poles). When the spectrum is not rational, or is rational with zeros, it will be necessary to approximate the infinite MFTF.

It is straightforward to generalize the results of Sections 3.1 and 3.2 to subspaces spanned by a finite number of translates of h_0 . In particular, if we replace the criteria of (11) and (13) by

$$\langle h_k, g_0 \rangle = 0 \quad -N \leq k \leq N, \quad k \neq 0 \quad (84)$$

for the ZFE and

$$\langle h_k, g_0 \rangle = 0 \quad 1 \leq k \leq N \quad (85)$$

for the DFE, we are left with the consideration of the finite dimensional subspaces $M(h_k, -N \leq k \leq N, k \neq 0)$ and $M(h_k, 1 \leq k \leq N)$, which we will write as M_N and M_N^+ respectively. Then the MFTF equalizers which satisfy (84) and (85) are similar to (54) and (55),

$$e_0(N) \triangleq h_0 - P(h_0, M_N) \quad (86)$$

$$e_0^+(N) \triangleq h_0 - P(h_0, M_N^+). \quad (87)$$

It is straightforward to see that Theorem 1 can be replaced by the following version:

Theorem 2: The following four statements are equivalent:

1. $h_0 \notin M_N$ [$h_0 \notin M_N^+$].
2. $\|e_0(N)\| > 0$ [$\|e_0^+(N)\| > 0$].
3. There exists a ZFE [DFE] in the restricted sense of (84) [(85)].
4. There exists an MFTF ZFE [DFE] in this restricted sense.

The question of when it can be asserted that $\|e_0(N)\| > 0$ and $\|e_0^+(N)\| > 0$ deserves consideration. The condition that $h_0 \in M_N^+$ requires that coefficients $\{\alpha_m, 1 \leq m \leq N\}$ exist which satisfy

$$h_0 = \sum_{m=1}^N \alpha_m h_m. \quad (88)$$

This occurrence will be precluded if the set $\{h_m, -\infty < m < \infty\}$ is

linearly independent. Similarly, linear independence is sufficient for a ZFE to exist in the sense of (84). The following lemma, which is proven in Appendix B, establishes sufficient conditions for the linear independence of $\{h_m, -\infty < m < \infty\}$:

Lemma 1: The following two conditions are sufficient for the linear independence of $\{h_m, -\infty < m < \infty\}$:

1. $\|e_0\| > 0$ or $\|e_0^+\| > 0$.
2. There exists an interval $[a, b]$, $a < b$, such that $R(\omega) > 0$, $\omega \in [a, b]$.

The first condition of Lemma 1 satisfies our intuition that if an infinite MFTF ZFE or DFE exists then the finite MFTF version should also exist. The second condition assures us that the finite equalizers also exist under much weaker conditions.

The following theorem establishes a relationship between the finite and infinite equalizers, and is proven in Appendix B:

Theorem 3: As $N \rightarrow \infty$, $\|e_0(N)\|^2$ is monotonically decreasing and approaches $\|e_0\|^2$, and likewise for $e_0^+(N)$. Furthermore, $\|e_0(N) - e_0\|^2 \rightarrow 0$ and $\|e_0^+(N) - e_0^+\|^2 \rightarrow 0$.

The primary conclusion of Theorem 3 is that the infinite equalizer can be approximated with arbitrary accuracy (in the sense of L_2 convergence) by a finite equalizer. In addition, it asserts that the S/N ratio of this finite equalizer is greater than that of the infinite equalizer; however, this desirable property may be entirely or partially offset by any residual intersymbol interference.

Each member of the sequence of equalizers guaranteed by Theorem 3 has different tap-gains, because the projection on a different subspace is being taken with each N . A more aesthetically pleasing approximation results when (58) and (59) are valid, for then

$$\left\| h_0 - \sum_{k=-N}^N a_k h_k - e_0 \right\| \rightarrow 0, \quad (89)$$

$$\left\| h_0 - \sum_{k=1}^N a_k^+ h_k - e_0^+ \right\| \rightarrow 0, \quad (90)$$

by the definition of convergence of the infinite sums in (58)–(59). Each succeeding equalizer defined by (89)–(90) is obtained by adding an additional tap, without changing the other tap-gains. As observed by Doob (Ref. 3, p. 564), a convergent sum of the form of (58)–(59) does not always exist; the following theorem gives sufficient conditions

for the validity of (58)–(59) which are generally satisfied in practical problems:

Theorem 4[†]: If there exist constants K_1 and K_2 , $0 < K_1 \leq K_2$, such that $K_1 \leq R(\omega) \leq K_2$, $|\omega| < \pi/T$, then convergent expansions of e_0 and e_0^+ of the form of (58)–(59) exist. Furthermore, the coefficients of the expansions are unique.

This theorem is proven in Appendix B. The question of uniqueness of the tap-gains of the DFE is one which was not answered by Price.⁶

Finally, the white output noise property of the MFTF DFE also extends to a finite MFTF DFE in the following sense: If the reception of (1) extends from N_1 to N_2 , where N_2 (but not necessarily N_1) is finite, then the DFE defined by

$$e_k^+ = h_k - P[h_k, M(h_m, k + 1 \leq m \leq N_2)]$$

will have white output noise samples. This fact is easily verified from the same containment of subspaces that was used in the proof for the infinite case.

IV. EXTENSION TO NONSTATIONARY NOISE AND CHANNEL

The previous sections have considered only the case where the additive noise is white. The extension to colored Gaussian noise can be handled in a straightforward fashion with the addition of a whitening filter. In this section we will generalize the ZFE and DFE to the case of arbitrary nonstationary second-order Gaussian noise (which includes colored Gaussian noise as a special case) using the techniques of reproducing kernel Hilbert space (RKHS).¹¹ Although the cases for which the corresponding RKHS can be characterized explicitly correspond generally to those cases which can be handled by other techniques, the RKHS approach does allow us to treat all cases simultaneously and concisely. In addition, it enables us to generalize simultaneously to an arbitrary nonstationary channel (to be precise, a channel which is changing in time in a deterministic and known fashion) with no additional complications. Perhaps the most interesting outcome of this effort will be the observation that the DFE white output noise property (discussed in Section 3.3) remains valid in this general case. The result is an interesting generalization of Forney's whitened matched filter.¹²

[†] Theorem 4 remains valid under the weaker hypothesis that $0 < \text{ess inf } R(\omega)$ and $\text{ess sup } R(\omega) < \infty$.

To this end, modify (1) to

$$r(t) = \sum_{m=N_1}^{N_2} B_m h_m(t) + n(t), \quad (91)$$

where, as before, N_1 and N_2 can be infinite. The noise will be assumed to be Gaussian with arbitrary autocorrelation

$$K(t, s) = E[n(t)n(s)]. \quad (92)$$

The subscript m on $h_m(t)$ indicates that the received pulses need not be translates of the same elementary waveform. The reception will be termed *channel stationary* when

$$h_m(t) = h(t - mT)$$

and *noise stationary* when

$$K(t, s) = K(t - s).$$

We denote by $L_2(n)$ the subspace of the Hilbert space of square integrable random variables spanned by $n(t)$, $-\infty < t < \infty$. This subspace is entirely analogous to $M(X_k, -\infty < k < \infty)$ defined earlier, except that the underlying parameter t is continuous. The following lemma is applicable:¹¹

Lemma 2: Let $H(K)$ consist of all functions $g(\cdot)$ of the form

$$g(\cdot) = E[n(\cdot)U] \quad (93)$$

for some $U \in L_2(n)$. Then $H(K)$ is a Hilbert space with inner product

$$\langle g, g \rangle_{H(K)} = E|U|^2. \quad (94)$$

The mapping $\psi: L_2(n) \rightarrow H(K)$ defined by (93) is a congruence which maps $n(t)$ into $K(\cdot, t)$.

The Hilbert space $H(K)$ defined by Lemma 2 is known as the reproducing kernel Hilbert space with reproducing kernel K . It is straightforward to show from (93) and (94) that $H(K)$ has the properties

$$K(\cdot, t) \in H(K), \quad -\infty < t < \infty, \quad (95)$$

$$\langle g(\cdot), K(\cdot, t) \rangle_{H(K)} = g(t), \quad g \in H(K). \quad (96)$$

It can be shown¹¹ that for any symmetric positive-definite kernel K there exists a unique Hilbert space satisfying (95)–(96).

The inverse of $g(\cdot)$ under ψ is usually given the suggestive notation

$$\langle g, n \rangle_{H(K)} \triangleq \psi^{-1}(g) \quad (97)$$

even though $n \notin H(K)$ with probability one and therefore (97) cannot be given an interpretation as an inner product.

It will be assumed that $h_m(t) \in H(K)$, since otherwise the detection problem is singular.[†] In nonstationary noise the space $H(K)$ takes the place of L_2 in the earlier white noise problem. Accordingly, we restrict the class of filters under consideration to $H(K)$ inner products with elements of $H(K)$. Thus, a filter can be written in the form

$$\langle g, r \rangle_{H(K)} = \sum_{m=-N_1}^{N_2} B_m \langle g, h_m \rangle_{H(K)} + \langle g, n \rangle_{H(K)}, \quad (98)$$

where the noise term in (98) assumes the special meaning of (97). Analogously to (15), we define the pulse autocorrelation

$$R(m, n) = \langle h_m, h_n \rangle_{H(K)}. \quad (99)$$

When the reception is noise and channel stationary, $R(m, n)$ is a function of the difference of its arguments, as in (15). In general, however, it is an arbitrary symmetric positive definite function defined for $N_1 \leq m, n \leq N_2$.[‡]

In the white noise case, we saw that the subspace of L_2 spanned by translates of $h(t)$ was congruent to the subspace of second-order random variables spanned by a wide-sense stationary random process. In the nonstationary noise case, the subspace of $H(K)$ spanned by h_m , $N_1 \leq m \leq N_2$, is congruent to the subspace of the second-order random variables spanned by a possibly nonstationary second-order random process. In the white noise case the theory of minimum mean-square error estimation of a wide-sense stationary random process was relevant; in the present case the random process becomes nonstationary. As before, the ZFE and DFE have interpretations as interpolation and prediction errors of the corresponding random process with autocorrelation $R(m, n)$. However, rather than pursue these correspondences further (in view of our results for the white noise case they are obvious), we will directly pursue the theory of the ZFE and DFE for the detection of B_m , $N_1 \leq m \leq N_2$, from $r(t)$ in (91).

[†] A singular detection problem is one in which a decision can be made which is correct with probability one.

[‡] The positive definite property follows from the inequality

$$0 \leq \left\| \sum_{m=1}^N \alpha_m h_{k_m} \right\|_{H(K)}^2 = \sum_{m=1}^N \sum_{n=1}^N \alpha_m \alpha_n R(k_m, k_n).$$

The theory of Section 3.1 remains valid if the subspaces $M(h_m, m \in I)$ are considered as subspaces of $H(K)$ rather than L_2 .[†] As before, the condition which is necessary and sufficient for the existence of a ZFE or DFE is that

$$h_k \notin M(h_m, m \in I).$$

The analogs of the MFTF versions of the DFE and ZFE are the elements given by (54) and (55), except that now we must work with e_k and e_k^+ instead of e_0 and e_0^+ (e_k is no longer necessarily simply a time translate of e_0 , etc.). A derivation similar to that given in Section 3.3 establishes that e_k and e_k^+ maximize the S/N ratio as before. In particular, when the filter of (91) is restricted to be a ZFE, (91) becomes

$$\langle g, \tau \rangle_{H(K)} = B_k \langle g, h_k \rangle_{H(K)} + \langle g, n \rangle_{H(K)} \quad (100)$$

and the S/N ratio is proportional to

$$S/N \propto \frac{\langle g, h_k \rangle_{H(K)}^2}{\langle g, g \rangle_{H(K)}} \leq \langle e_0, e_0 \rangle_{H(K)} \quad (101)$$

since the variance of the noise term in (100) is, from (97),

$$\begin{aligned} E |\langle g, n \rangle_{H(K)}|^2 &\triangleq E |\psi^{-1}(g)|^2 \\ &= \langle g, g \rangle_{H(K)} \end{aligned}$$

through the congruence established in Lemma 2. Equation (101) demonstrates that the MFTF ZFE maximizes the S/N ratio, and the same result follows for the DFE by the same method.

A general equation can be given for the projection element required for the MFTF. This equation is entirely analogous to a result of Parzen¹¹ for stochastic estimation. To this end we require a lemma which is a restatement of Lemma 2:

Lemma 3: Let $H(R)$ consist of all functions $f(m)$, $m \in I$, of the form

$$f(m) = \langle h_m, F \rangle_{H(K)} \quad m \in I \quad (102)$$

for some $F \in M(h_m, m \in I)$. Then $H(R)$ is the RKHS with reproducing kernel $R(m, n)$, $m, n \in I$, and has inner product

$$\langle f, f \rangle_{H(R)} = \langle F, F \rangle_{H(K)}. \quad (103)$$

The mapping $\phi: M(h_m, m \in I) \rightarrow H(R)$ defined by (102) is a congruence which maps h_m into $R(\cdot, m)$.

[†] We use I as a set of indices to avoid repeating the equations twice. For the ZFE, $I = [N_1, k-1] \cup [k+1, N_2]$ and for the DFE $I = [k+1, N_2]$. For the infinite case, $N_2 = -N_1 = \infty$. The digit B_k is being detected.

The reader might find it instructive to verify from (102)–(103) that the RKHS properties hold for $H(R)$,

$$R(\cdot, n) \in H(R), \quad (104)$$

$$\langle f(\cdot), R(\cdot, n) \rangle_{H(R)} = f(n), \quad (105)$$

where $f(\cdot) \in H(R)$.

The problem we want to attack is finding the projection P of some vector Q on $M(h_m, m \in I)$ (later we will let $Q = h_k$). From (3) we have

$$\langle Q - P, h_m \rangle_{H(K)} = 0, \quad m \in I \quad (106)$$

or

$$\langle P, h_m \rangle_{H(K)} = \rho_Q(m), \quad m \in I, \quad (107)$$

where

$$\rho_Q(m) \triangleq \langle Q, h_m \rangle_{H(K)}, \quad m \in I. \quad (108)$$

In (107), $\rho_Q(m)$ is a known function and P is to be determined. Assuming for the moment that $\rho_Q \in H(R)$, from Lemma 3 we see that ρ_Q is the image of P under the congruence ϕ , and hence

$$P = \phi^{-1}(\rho_Q), \quad (109)$$

which is the solution we desire. Using the congruence properties of ϕ , the length of $Q - P$ is

$$\begin{aligned} \|Q - \phi^{-1}(\rho_Q)\|_{H(K)}^2 &= \|Q\|_{H(K)}^2 - 2\langle Q, \phi^{-1}(\rho_Q) \rangle_{H(K)} + \|\phi^{-1}(\rho_Q)\|_{H(K)}^2 \\ &= \|Q\|_{H(K)}^2 - \|\rho_Q\|_{H(R)}^2. \end{aligned} \quad (110)$$

Establishing that in fact $\rho_Q \in H(R)$ is straightforward. Note that

$$\begin{aligned} \rho_Q(m) &= \langle Q, h_m \rangle_{H(K)} \\ &= \langle Q - P, h_m \rangle_{H(K)} + \langle P, h_m \rangle_{H(K)} \\ &= \langle P, h_m \rangle_{H(K)}, \end{aligned} \quad (111)$$

which implies that $\rho_Q \in H(R)$ by Lemma 3 since $P \in M(h_m, m \in I)$.

Replacing Q by h_k in (109), we get the desired projection

$$P[h_k, M(h_m, m \in I)] = \phi^{-1}[R(k, \cdot)] \quad (112)$$

The ZFE and DFE are obtained by letting I equal the appropriate set. The S/N ratios of the receivers are proportional to, from (101) and (110),

$$\text{S/N} \propto \|h_k\|_{H(K)}^2 - \|R(k, \cdot)\|_{H(R)}^2. \quad (113)$$

The RKHS approach has reduced the problem to that of finding

RKHS inner products. In some cases these inner products can be explicitly characterized, while in all others they can be determined by convergent iterative techniques.¹¹

We can also quickly show that the DFE white output noise property discussed in Section 3.3 generalizes. From (98), the noise samples at the filter output are

$$\begin{aligned} n_k &= \langle e_k^+, n \rangle_{H(K)} \\ &= \psi^{-1}(e_k^+) \end{aligned} \quad (114)$$

by definition. From (114) and Lemma 2,

$$\begin{aligned} E(n_j n_k) &= E[\psi^{-1}(e_j^+) \psi^{-1}(e_k^+)] \\ &= \langle e_j^+, e_k^+ \rangle_{H(K)} \\ &= 0, \quad j \neq k \end{aligned} \quad (115)$$

by the same reasoning as before.

Finally, it is instructive to demonstrate that this RKHS formulation reduces to the whitening filter approach when the reception is noise and channel stationary. Assume that

$$K(t, s) = \frac{1}{2\pi} \int_{-\infty}^{\infty} e^{j\omega(t-s)} N(\omega) d\omega, \quad (116)$$

where $N(\omega)$ is uniformly bounded and never vanishes. Under these conditions we claim that $H(K)$ consists of all integrable $g(t)$ with Fourier transforms $G(\omega)$ which satisfy

$$\|g\|_{H(K)}^2 = \frac{1}{2\pi} \int_{-\infty}^{\infty} |G(\omega)|^2 \frac{1}{N(\omega)} d\omega. \quad (117)$$

To verify this, properties (95)–(96) must be checked. Equation (95) is valid since $N(\omega)$ is integrable, while (96) follows from

$$\begin{aligned} \langle g(\cdot), K(\cdot, t) \rangle_{H(K)} &= \frac{1}{2\pi} \int_{-\infty}^{\infty} G(\omega) [e^{-j\omega t} N(\omega)]^* \frac{1}{N(\omega)} d\omega \\ &= \frac{1}{2\pi} \int_{-\infty}^{\infty} G(\omega) e^{j\omega t} d\omega \\ &= g(t), \end{aligned} \quad (118)$$

where (*) denotes complex conjugation. From (117), the $H(K)$ inner product consists of a filter with frequency response $N^{-1}(\omega)$ (which is the whitening filter) followed by an ordinary L_2 inner product, and is therefore consistent with the whitening filter formulation.

V. CONCLUSIONS

This paper has presented a unified and rather thorough treatment of the ZFE and DFE. In a companion paper,⁷ the geometric model of intersymbol interference developed here will be used to study the minimum distance problem encountered in the performance analysis of the maximum likelihood detector¹² and in evaluating a lower bound on the performance of any receiver.¹⁴ It is shown there that a canonical relationship exists between the minimum distance and the performance and tap-gains of the MFTF DFE.

No performance example comparing the DFE and ZFE on a channel of practical interest has been given in this paper in order that the maximum likelihood detector may enter into the comparison. In Ref. 7 the performance of three receivers is calculated for a channel whose loss in dB increases as the square-root of frequency. This channel is an excellent model of coaxial cable and some types of wire-pairs.

VI. ACKNOWLEDGMENTS

The author is indebted to R. Price for many valuable comments. In particular, it was he who suggested the extension to nonstationary noise using RKHS theory. The author also appreciates many valuable discussions with D. L. Duttweiler.

APPENDIX A

The purpose of this appendix is to derive an approximation to the Fourier coefficients of (48) in terms of discrete Fourier transform (DFT), which can be efficiently evaluated using the FFT algorithm.

Define a normalized function

$$F(\lambda) = \log \frac{R\left(\frac{2\pi}{T}\lambda\right)}{T} \quad (119)$$

so that

$$r_n = \frac{1}{2} \int_{-\frac{1}{2}}^{\frac{1}{2}} e^{-jn2\pi\lambda} F(\lambda) d\lambda. \quad (120)$$

Approximating the integral by a summation,

$$\begin{aligned} \hat{r}_n &\cong \frac{1}{2N} \sum_{k=0}^{N-1} F\left(\lambda_0 + \frac{k}{N} - \frac{1}{2}\right) e^{-jn2\pi(\lambda_0+k/N-\frac{1}{2})} \\ &= \frac{1}{2} e^{-jn2\pi(\lambda_0-\frac{1}{2})} \frac{1}{N} \sum_{k=0}^{N-1} F\left(\lambda_0 + \frac{k}{N} - \frac{1}{2}\right) e^{-j2\pi(kn/N)}, \quad (121) \end{aligned}$$

where the sum on the right is a discrete Fourier transform.

In order to determine the effect of this approximation, substitute

$$\frac{1}{2}F(\lambda) = \sum_k r_k e^{jk2\pi\lambda} \tag{122}$$

into the approximation equation (121) to yield

$$\begin{aligned} \hat{r}_n &= \sum_{m=-\infty}^{\infty} r_m \frac{1}{N} \sum_{k=0}^{N-1} e^{j(m-n)2\pi(\lambda_0+k/N-k)} \\ &= r_n + \sum_{l \neq 0} e^{j2\pi l N \lambda_0} (-1)^l r_{n+lN}. \end{aligned} \tag{123}$$

Thus, the approximation of (121) yields the desired Fourier coefficient plus the sum of alias terms. N must be larger than the number of coefficients to be evaluated and large enough that the alias terms r_{n+lN} are small. In practice, $N \cong 5,000$ can be achieved with modest amounts of computer time using the FFT algorithm.

APPENDIX B

Proofs of Theorems

Proof of Lemma 1: Since $\|e_0^+\|^2 \geq \|e_0\|^2$ it suffices to show that $\|e_0^+\| > 0$ implies that $\{h_m, -\infty < m < \infty\}$ is linearly independent set. To this end, assume that

$$\left\| \sum_{m=1}^N \alpha_m h_{k_m} \right\|^2 = 0, \quad k_1 < k_2 < \dots < k_N. \tag{124}$$

To show that $\alpha_1 = 0$, assume to the contrary that $\alpha_1 \neq 0$ and note that

$$0 = |\alpha_1|^2 \left\| h_{k_1} + \sum_{m=2}^N \frac{\alpha_m}{\alpha_1} h_{k_m} \right\|^2 \geq |\alpha_1|^2 \|e_0^+\| > 0. \tag{125}$$

This contradiction establishes that $\alpha_1 = 0$. Continuing by induction in the same fashion, it can be shown that $\alpha_m = 0, 1 \leq m \leq N$.

To show that the second condition of Lemma 1 implies linear independence, we use a proof similar to Tuft's.¹³ By the congruence of (22), (124) is equivalent to

$$\int_{-\pi/T}^{\pi/T} \left| \sum_{m=1}^N \alpha_m e^{-j\omega k_m T} \right|^2 R(\omega) d\omega = 0,$$

which implies that the integrand is zero almost everywhere on $[a, b]$. This is impossible unless $\alpha_m = 0, 1 \leq m \leq N$, since otherwise

$$\left| \sum_{m=1}^N \alpha_m e^{-j\omega k_m T} \right|^2$$

has at most a finite number of algebraic zeros on $[a, b]$ and $R(\omega)$ is strictly positive.

Proof of Theorem 3: We will prove the result for the ZFE; the proof for the DFE is identical. Since for $N \leq M$

$M(h_k, |k| \leq N, k \neq 0) \subset M(h_k, |k| \leq M, k \neq 0) \subset M(h_k, k \neq 0)$, the inequality

$$\|e_0\| \leq \|e_0(M)\| \leq \|e_0(N)\|$$

follows. Hence $\|e_0(M)\|^2$ must approach a limit,

$$\lim_{N \rightarrow \infty} \|e_0(N)\| \geq \|e_0\|.$$

Denote by the shortened notation P the projection of h_0 on $M(h_k, k \neq 0)$ (so that $e_0 \triangleq h_0 - P$). Since $P \in M(h_k, k \neq 0)$, there exists a sequence $\gamma_n \in M(h_k, |k| \leq n, k \neq 0)$ such that $\gamma_n \rightarrow P$ and we have

$$\|h_0 - \gamma_n\|^2 = \|e_0\|^2 + \|P - \gamma_n\|^2.$$

For any $\epsilon > 0$, there exists an $N(\epsilon)$ such that

$$\|h_0 - \gamma_n\|^2 \leq \|e_0\|^2 + \epsilon$$

for $n \geq N(\epsilon)$, and since $\|e_0(n)\|^2 \leq \|h_0 - \gamma_n\|^2$ we have

$$\|e_0\|^2 \leq \|e_0(n)\|^2 \leq \|e_0\|^2 + \epsilon,$$

which establishes that $\|e_0(n)\| \rightarrow \|e_0\|$. The remainder of the proof follows that of the projection theorem. By the parallelogram law,

$$\|e_0(N) - e_0\|^2 = 2\|e_0(N)\|^2 + 2\|e_0\|^2 - \|e_0(N) + e_0\|^2,$$

but defining $P(N) = P[h_0, M(h_k, |k| \leq N, k \neq 0)]$

$$\begin{aligned} \|e_0(N) + e_0\|^2 &= \|h_0 - P(N) + h_0 - P\|^2 \\ &= 4 \left\| h_0 - \frac{P(N) + P}{2} \right\|^2 \geq 4\|e_0\|^2, \end{aligned}$$

we have

$$\|e_0(N) - e_0\|^2 \leq 2[\|e_0(N)\|^2 - \|e_0\|^2] \rightarrow 0.$$

Proof of Theorem 4: From (22) we have

$$\left| \left| \sum_{m=1}^N \beta_m h_{km} \right| \right|^2 = \frac{1}{2\pi} \int_{-\pi/T}^{\pi/T} \left| \sum_{m=1}^N \beta_m e^{-j\omega kmT} \right|^2 R(\omega) d\omega.$$

A standard result of Toeplitz theory asserts that

$$\frac{1}{T} \left\{ \sum_{m=1}^N |\beta_m|^2 \right\} \text{ess inf } R(\omega) \leq \left\| \sum_{m=1}^N \beta_m h_k \right\|^2$$

$$\forall \frac{1}{T} \left\{ \sum_{m=1}^N |\beta_m|^2 \right\} \text{ess sup } R(\omega).$$

The conclusions of the theorem then follow from Theorem 5.17.18 of Ref. 10.

REFERENCES

1. Wozencraft, J. M., and Jacobs, I. M., *Principles of Communication Engineering*, New York: Wiley, 1967.
2. Grenander, U., and Rosenblatt, M., *Statistical Analysis of Stationary Time Series*, New York: Wiley, 1957.
3. Doob, J. L., *Stochastic Processes*, New York: Wiley, 1953.
4. Lucky, R. W., Salz, J., and Weldon, E. J., *Principles of Data Communication*, New York: McGraw-Hill, 1968.
5. Monsen, P., "Linear Equalization for Digital Transmission over Noisy Dispersive Channels," Ph.D. Dissertation, Columbia University, June 1970.
6. Price, R., "Nonlinearly Feedback-Equalized PAM vs Capacity for Noisy Filter Channels," 1972, Int. Conf. Commun., Philadelphia, June 1972.
7. Messerschmitt, D. G., "A Geometric Theory of Intersymbol Interference. Part II: Performance of the Maximum Likelihood Detector," B.S.T.J., this issue, pp. 1521-1539.
8. Messerschmitt, D. G., "A Unified Geometric Theory of Zero-Forcing and Decision-Feedback Equalization," 1973 Int. Conf. Commun., Seattle, June 1973.
9. Messerschmitt, D. G., "Digital Communications: Detectors and Estimators for the Time-Varying Channel with Intersymbol Interference," Ph.D. Dissertation, University of Michigan, December 1971.
10. Naylor, A. W., and Sell, G. R., *Linear Operator Theory in Science and Engineering*, New York: Holt, Rinehart and Winston, 1971.
11. Parzen, E., *Time Series Analysis Papers*, San Francisco: Holden-Day, 1967.
12. Forney, G. D., Jr., "Maximum Likelihood Sequence Estimation of Digital Sequences in the Presence of Intersymbol Interference," IEEE Trans. Inform. Theory, *IT-18*, May 1972, p. 363.
13. Tufts, D. W., "Nyquist's Problem—The Joint Optimization of Transmitter and Receiver in Pulse Amplitude Modulation," Proc. IEEE, *53*, March 1965.
14. Forney, G. D., Jr., "Lower Bounds on Error Probability in the Presence of Large Intersymbol Interference," IEEE Trans. Commun., *COM-20*, February 1972, p. 76.

A Geometric Theory of Intersymbol Interference

Part II: Performance of the Maximum Likelihood Detector

By D. G. MESSERSCHMITT

(Manuscript received May 24, 1973)

In a companion paper,¹ a geometric approach to the study of intersymbol interference was introduced. In the present paper this approach is applied to the performance analysis of the Viterbi algorithm maximum likelihood detector (MLD) of Forney.²⁻⁴ It is shown that a canonical relationship exists between the minimum distance, which Forney has shown determines the performance of the MLD, and the performance and tap-gains of the decision-feedback equalizer (DFE). Upper and lower bounds on the minimum distance are derived, as is an iterative technique for computing it exactly.

The performances of the MLD, DFE, and zero-forcing equalizer (ZFE) are compared on the \sqrt{f} channel representative of coaxial cables and some wire pairs. One important conclusion is that, previous statements notwithstanding,^{2,4} even the MLD experiences a substantial penalty in S/N ratio relative to the isolated pulse bound on this channel of practical interest.

I. INTRODUCTION

Forney^{2,3} has detailed the Viterbi algorithm version of the maximum likelihood detector (MLD) of digital sequences in the presence of intersymbol interference. He asserts that the probability of bit error of the MLD in additive white Gaussian noise can be bounded at high S/N ratios in the form

$$K_L Q \left(\frac{d_{\min}}{2\sigma} \right) \leq P_e \leq K_u Q \left(\frac{d_{\min}}{2\sigma} \right), \quad (1)$$

where K_L and K_u are constants, Q is the Gaussian distribution

function,

$$Q(x) = \frac{1}{\sqrt{2\pi}} \int_x^\infty e^{-y^2/2} dy, \quad (2)$$

d_{\min} is the minimum distance between any two transmitted signals (it will be defined more fully in Section 2.2), and σ^2 is the noise variance. For comparison purposes, the probability of error for a matched filter receiver in the absence of intersymbol interference is

$$P_e = Q\left(\frac{\sqrt{R_0}}{2\sigma}\right), \quad (3)$$

where R_0 is the energy of an isolated pulse [(1) reduces to (3) in this case].

Forney also asserts that the lower bound of (1) is also a lower bound on the error probability of any receiver.⁴ Thus, the MLD achieves, within the multiplicative constant K_u/K_L , the minimum probability of error attainable by any receiver at high S/N ratios, and, in a very fundamental sense, the quantity

$$d_{\min}^2/R_0$$

is a measure of the effective decrease in the S/N ratio (relative to the detection of an isolated pulse) resulting from intersymbol interference.

The determination of the quantity d_{\min}^2 (known as the "minimum distance problem") is therefore a very important one for, even if the implementation of the MLD is not contemplated on a particular channel, d_{\min}^2 is a measure of the potential performance which can be obtained using receivers of arbitrary complexity. Unfortunately, on channels with severe intersymbol interference, the exact analytical determination of d_{\min}^2 does not appear feasible because of the nonlinear nature of the problem.

The minimum distance can be determined numerically by the "brute force" technique of calculating a sequence of converging upper bounds. A shortcoming of this method is that it gives no assurance as to when convergence to the desired accuracy has occurred. In addition, it gives no insight into the nature of d_{\min}^2 and its relationship to the intersymbol interference or to the performances of other receivers.

In this paper, we attack the minimum distance problem using a geometric theory of intersymbol interference developed in companion papers.^{1,5} A canonical relationship will be shown between d_{\min}^2 and the decision-feedback equalizer (DFE). This relationship will be exploited

to derive simple lower and upper bounds on d_{\min}^2 in terms of the tap-gains of the DFE transversal filter and the S/N ratio performance of the DFE. In addition, an iterative procedure will be derived for the calculation of d_{\min}^2 to any desired accuracy using a sequence of converging upper and lower bounds on d_{\min}^2 . The lower bounds give us a measure of the degree of convergence and enable us to terminate the calculation when the desired accuracy is assured.

After consideration of the minimum distance problem in Section II, the performance of the zero-forcing equalizer (ZFE), DFE, and MLD is compared on a channel of practical interest in Section III.

II. PERFORMANCE OF THE MLD

The minimum distance problem will now receive consideration. The first step is to briefly review the notation of a companion paper.¹

2.1 Notation

The reception from a PAM communication channel takes the form

$$r(t) = \sum_k B_k h(t - kT) + n(t), \quad (4)$$

where each B_k assumes one of a finite number of predetermined values (the data being transmitted), $h(t)$ is square-integrable (element of L_2),* and $n(t)$ is white Gaussian noise.

When we denote $h(t - kT)$ as an element of L_2 by h_k , $M(h_k, k \in I)$ is the smallest closed linear subspace of L_2 containing all finite linear combinations of elements of the set $\{h_k, k \in I\}$. The projection of a vector x on $M(h_k, k \in I)$ is denoted by $P[x, M(h_k, k \in I)]$. The forward matched-filter transversal-filter combination of the DFE corresponds to the L_2 inner product of the reception $r(t)$ with the element

$$e_k^+ \triangleq h_k - P[h_k, M(h_m, m > k)] \quad (5)$$

and is orthogonal to the subspace $M(h_m, m > k)$. The quantity

$$\frac{\|e_0^+\|^2}{R_0},$$

where

$$R_k \triangleq \langle h_m, h_{m+k} \rangle \quad (6)$$

* We denote by L_2 the space of square integrable waveforms with inner product

$$\langle x, y \rangle = \int_{-\infty}^{\infty} x(t)y(t)dt$$

and norm $\|x\|^2 = \langle x, x \rangle$.

is the effective decrease in S/N ratio relative to an isolated pulse for the DFE. Thus, $\|e_0^+\|^2$ plays the same role for the DFE as d_{\min}^2 plays for the MLD.

The sequence of vectors $\{w_k \triangleq e_k^+ / \|e_k^+\|\}$ is an orthonormal sequence in L_2 , and h_n has the orthogonal expansion

$$h_n = \sum_{m=0}^{\infty} C_m w_{m+n}, \quad (7)$$

where the coefficients $\{C_m\}$ can be determined by the method of Ref. 1 for channels with either a rational or nonrational spectrum. In particular, we have

$$C_0 = \|e_0^+\|. \quad (8)$$

Of course, it is apparent that (7) is valid only as long as $\|e_0^+\| > 0$, which is true if and only if a DFE exists.

2.2 Interpretation of the Minimum Distance

The MLD described by Forney² consists of a combination of a matched filter followed by a causal or anticausal transversal filter, the combination of which he calls a "whitened matched filter," followed by a dynamic programming algorithm known as the Viterbi algorithm.³ The whitened matched filter forms a sequence of sufficient statistics for the detection of the data digits and has independent noise samples at the output. As pointed out by Price,⁴ the anticausal whitened matched filter is identical to the forward linear filter portion of the DFE.

The signal at the output of the whitened matched filter (or DFE forward filter) is¹

$$r_k = C_0^2 B_k + \sum_{m=1}^{\infty} C_0 C_m B_{k-m} + n_k, \quad (9)$$

where n_k is a noise sample. The DFE forms the quantity

$$r'_k = r_k - \sum_{m=1}^{\infty} C_0 C_m \hat{B}_{k-m} \quad (10)$$

and applies it to a decision threshold to determine the estimated digit \hat{B}_k . The MLD detector, on the other hand, assumes that the sum in (9) is truncated to M terms and determines the sequence $\{\hat{B}_k\}$ so as to minimize

$$\sum_{k=1}^N \left\{ r_k - \sum_{m=0}^M C_0 C_m \hat{B}_{k-m} \right\}^2. \quad (11)$$

Thus, the two receivers perform similar functions on the same sufficient statistics r_n , the major differences being the greater complexity of the MLD and the susceptibility of the DFE to decision errors. We will now demonstrate the less obvious conclusion that the *performance* of the MLD is closely related to the DFE as well.

The minimum distance, d_{\min}^2 , is defined as²

$$d_{\min}^2 \triangleq \inf_{\epsilon_0 \neq 0} \left\| \sum_{n=0}^N \epsilon_n h_n \right\|^2, \quad (12)$$

where the infimum is over all error sequences $(\epsilon_0, \dots, \epsilon_N)$ and all N .^{*} Each ϵ_k assumes the value $+1$, -1 , or zero (for simplicity, the binary case with $B_k = 1$ or 0 is considered). Thus, d_{\min} is the minimum distance in L_2 between two signals in the signal set. It is apparent that

$$d_{\min}^2 \leq R_0, \quad (13)$$

since R_0 corresponds to $\epsilon_n = 0$, $n > 0$. Thus, d_{\min}^2/R_0 , which is the S/N ratio penalty, is a number between zero and unity as it should be.

It is apparent in (12) that without loss of generality we can choose $\epsilon_0 = 1$ and write

$$d_{\min}^2 = \inf \left\| h_0 + \sum_{n=1}^N \epsilon_n h_n \right\|^2. \quad (14)$$

The sum in (14) is an element of $M(h_k, k \geq 1)$, and the minimization in (14) is an attempt to find the element of $M(h_k, k \geq 1)$ with manifold coefficients $(+1, -1, 0)$ which is closest (in \mathcal{L}_2 metric) to h_0 . We know that the closest element without the restriction in coefficients is the projection of h_0 on $M(h_k, k \geq 1)$, $P[h_0, M(h_k, k \geq 1)]$. Thus, intuitively, d_{\min}^2 is determined by how closely the projection can be approximated by an element with restricted manifold coefficients. To formalize this intuition, add and subtract the projection from (14) and utilize (5),

$$\begin{aligned} d_{\min}^2 &= \inf \left\| e_0^+ + P[h_0, M(h_k, k \geq 1)] + \sum_{n=1}^N \epsilon_n h_n \right\|^2 \\ &= \|e_0^+\|^2 + \inf \left\| P[h_0, M(h_k, k \geq 1)] + \sum_{n=1}^N \epsilon_n h_n \right\|^2, \end{aligned} \quad (15)$$

where the fact that e_0^+ is orthogonal to $M(h_k, k > 0)$ has been used to eliminate the cross-product in (15). The most immediate consequence of (15) is that

$$d_{\min}^2 \geq \|e_0^+\|^2. \quad (16)$$

^{*} In most cases of interest, the infimum will be achieved for finite N .

We have thus succeeded in proving formally what should be obvious from considerations of the relative complexity of the two receivers: The effective S/N ratio of the MLD always exceeds that of the DFE (and hence ZFE[†]).^{*} The second consequence of (15) is the formalization of our intuition through the assertion that the amount by which the S/N ratio of the MLD exceeds that of the DFE is governed by the coarseness of the best approximation to the projection by the element with restricted coefficients: The poorer the approximation, the better the S/N ratio of the MLD.

Writing the projection in the form

$$P[h_0, M(h_k, k > 0)] = - \sum_{m=1}^{\infty} a_m^+ h_m, \quad (17)$$

we note that the a_m^+ are the tap-gains of the DFE forward transversal filter, and rewrite (15) as[†]

$$d_{\min}^2 = \|e_0^+\|^2 + \inf \left\| \sum_{n=1}^{\infty} (\epsilon_n - a_n^+) h_n \right\|^2. \quad (18)$$

Equation (18) shows the fundamental relationship between the minimum distance, the effective S/N ratio of the DFE (in the form of $\|e_0^+\|^2$), and the tap-gains of the DFE transversal filter. In particular, we can assert that $d_{\min}^2 = \|e_0^+\|^2$ if and only if the tap-gains are all +1, -1, or zero.

2.3 Bounds on the Minimum Distance

Equation (18) can be used to derive bounds on d_{\min}^2 in terms of the DFE tap-gains. From the identity[†]

$$\left\| \sum_{n=1}^N (\epsilon_n - a_n^+) h_n \right\|^2 = (\epsilon_k - a_k^+)^2 \left\| h_k + \sum_{\substack{n=1 \\ n \neq k}}^N \frac{\epsilon_n - a_n^+}{\epsilon_k - a_k^+} h_n \right\|^2, \quad (19)$$

we immediately get the bounds

$$\left\| \sum_{n=1}^N (\epsilon_n - a_n^+) h_n \right\|^2 \geq \begin{cases} (\epsilon_1 - a_1^+)^2 \|e_0^+\|^2, & k = 1 \\ (\epsilon_k - a_k^+)^2 \|e_0\|^2, & k > 1, \end{cases} \quad (20)$$

^{*} We are tempted to argue that (16) is implied by the assertion in Ref. 2 that the MLD achieves the lowest effective S/N ratio of any receiver. However, that is not the case, because of the effect of decision errors on the DFE. The effective S/N ratio of the DFE could be higher than that of the MLD, and yet the DFE could have at the same time a higher error probability because of error propagation.

[†] We have taken the liberty of writing a sum over infinite error sequences, where it is understood that the infimum is only over error sequences with a finite number of nonzero terms.

[‡] In (19) it is assumed that $(\epsilon_k - a_k^+) \neq 0$. When $\epsilon_k - a_k^+ = 0$, (20) is trivially satisfied.

since

$$\sum_{\substack{n=1 \\ n \neq k}}^N \frac{(\epsilon_n - a_n^+)}{(\epsilon_k - a_k^+)} h_n$$

is an element of $M(h_m, m \neq k)$. In (20), e_0 is the ZFE filter defined in Ref. 1,

$$e_0 \triangleq h_0 - P[h_0, M(h_k, k \neq 0)]. \tag{21}$$

In addition, if we define $\lambda_{\min}(N)$ and $\lambda_{\max}(N)$ as the minimum and maximum eigenvalues of the correlation matrix

$$\mathbf{R}_N \triangleq [R_{m-n}] \quad 1 \leq m, n \leq N,$$

then we can assert that

$$\lambda_{\min}(N) \sum_{n=1}^N (\epsilon_n - a_n^+)^2 \leq \left\| \sum_{n=1}^N (\epsilon_n - a_n^+) h_n \right\|^2 \leq \lambda_{\max}(N) \sum_{n=1}^N (\epsilon_n - a_n^+)^2. \tag{22}$$

A standard Toeplitz form result⁷ asserts that*

$$\lim_{N \rightarrow \infty} \lambda_{\min}(N) = \frac{1}{T} \text{ess inf } R(\omega)$$

$$\lim_{N \rightarrow \infty} \lambda_{\max}(N) = \frac{1}{T} \text{ess sup } R(\omega).$$

Applying (18), (20), and (22), we get three lower and one upper bound on d_{\min}^2 in terms of the tap coefficients of the DFE,

$$d_{\min}^2 \geq \|e_0^+\|^2 + \begin{cases} \|e_0^+\|^2 \min_{\epsilon_1} (\epsilon_1 - a_1^+)^2 \\ \|e_0\|^2 \min_{\epsilon_k} (\epsilon_k - a_k^+)^2, & k > 1 \\ \frac{1}{T} \{ \text{ess inf } R(\omega) \} \lim_{N \rightarrow \infty} \min_{\epsilon_1, \dots, \epsilon_N} \sum_{n=1}^N (\epsilon_n - a_n^+)^2 \end{cases}$$

$$d_{\min}^2 \leq \|e_0^+\|^2 + \frac{1}{T} \{ \text{ess sup } R(\omega) \} \lim_{N \rightarrow \infty} \min_{\epsilon_1, \dots, \epsilon_N} \sum_{n=1}^N (\epsilon_n - a_n^+)^2. \tag{23}$$

In addition, an upper bound can be obtained by substituting any error sequence into (18); a reasonable choice is

$$\epsilon_k = \begin{cases} +1, & a_k^+ < -\frac{1}{2} \\ 0, & -\frac{1}{2} < a_k^+ < \frac{1}{2} \\ -1, & a_k^+ > \frac{1}{2} \end{cases}. \tag{24}$$

* For all practical purposes, "ess inf" and "ess sup" can be replaced by "min" and "max," respectively.

These five bounds can be useful in estimating the penalty in S/N ratio for the MLD. They all require the existence of a DFE and require that the projection can be written as the convergent sum of (17).^{*} The second and third bounds of (23) are an improvement on (16) only when the increasingly stringent requirements that a ZFE exist ($\|e_0\| > 0$) and $R(\omega)$ be uniformly bounded away from zero (almost everywhere) are imposed. The requirement of the upper bound of (23) that $R(\omega)$ be uniformly upper bounded (almost everywhere) will generally be satisfied in practice. All the bounds require a pointwise minimization over error sequences, a task much simpler than minimizing (12) directly.

As a simple application of these bounds, consider the exponential autocorrelation

$$R_k = A^{|k|}, \quad 0 < A < 1. \quad (25)$$

Then we have^{1,2}

$$d_{\min}^2 = \begin{cases} 1, & 0 < A \leq \frac{1}{2} \\ 2(1 - A), & \frac{1}{2} < A < 1 \end{cases} \quad (26)$$

$$\|e_0\|^2 = (1 - A^2)/(1 + A^2)$$

$$\|e_0^+\|^2 = 1 - A^2$$

$$a_1^+ = -A, \quad a_k^+ = 0, \quad k > 1.$$

The first and third bounds of (23) become

$$d_{\min}^2 \geq \begin{cases} 1 - A^4, & 0 < A \leq \frac{1}{2} \\ (1 - A^2)(2 + A^2 - 2A), & \frac{1}{2} < A < 1 \end{cases} \quad (27)$$

$$d_{\min}^2 \geq \begin{cases} 1 - 2A^3/(1 + A), & 0 < A \leq \frac{1}{2} \\ 2(1 - A)(1 + A^2)/(1 + A), & \frac{1}{2} < A < 1 \end{cases} \quad (28)$$

and the upper bound of (23) becomes

$$d_{\min}^2 \leq \begin{cases} 1 + \frac{2A^3}{1 - A}, & 0 < A \leq \frac{1}{2} \\ 2(1 - A^2), & \frac{1}{2} < A < 1. \end{cases} \quad (29)$$

These bounds are plotted in Fig. 1. The upper bound of (24) is equal to d_{\min}^2 and is not plotted.

^{*} If the projection of h_0 on $P(h_k, k \geq 1)$ cannot be written in the form of (17), the bounds of (22) to (24) can be fixed up by considering the projection on $P(h_k, 1 \leq k \leq N)$ and taking limits as $N \rightarrow \infty$. The tap-gains will then be a function of N , and the process will be more difficult.

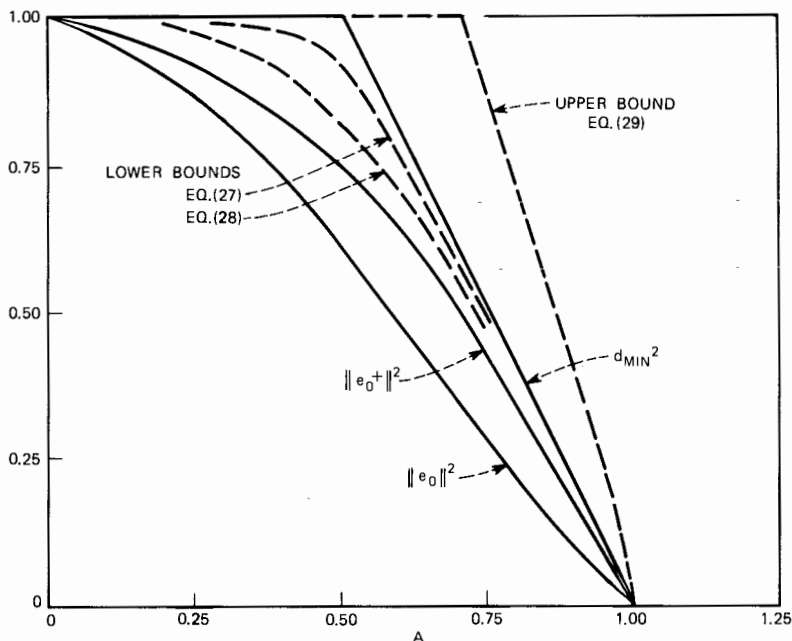


Fig. 1—Bounds on d_{\min}^2 for an exponential autocorrelation.

The bounds just determined have the disadvantages that (i) they require calculation of the DFE tap coefficients and (ii) they do not give precise results on d_{\min}^2 . The exact value of d_{\min}^2 can be determined numerically by the direct minimization of (12); by letting $N \rightarrow \infty$ while exhaustively minimizing over error sequences, we get a sequence of upper bounds on d_{\min}^2 which approach d_{\min}^2 monotonically. The obvious difficulty with this method is that the number of error sequences which must be checked grows as 3^N , and the computational effort soon becomes unreasonable. What happens in practice is that the true minimum is achieved for a finite (and small) N . However, unless we have some method of determining when the true minimum is reached, there must always remain a degree of uncertainty as to whether the true minimum has been reached.

Our approach to this computational problem will be to derive a sequence of *lower* bounds on d_{\min}^2 which also approach d_{\min}^2 monotonically. We can then halt the process at a value of N where the upper and lower bounds are close enough to ensure knowledge of d_{\min}^2 within the desired accuracy. To this end, we will utilize the orthogonal expansion

of (7). Substituting (7) into the sum of (12),

$$\begin{aligned}\sum_{n=0}^{\infty} \epsilon_n h_n &= \sum_{n=0}^{\infty} \epsilon_n \sum_{m=0}^{\infty} C_m w_{n+m} \\ &= \sum_{m=0}^{\infty} \beta_m w_m,\end{aligned}\quad (30)$$

where

$$\beta_m = \sum_{k=0}^m \epsilon_k C_{m-k}.\quad (31)$$

Then, because the $\{w_n\}$ are orthonormal,

$$\left\| \sum_{n=0}^{\infty} \epsilon_n h_n \right\|^2 = \sum_{n=0}^{\infty} \beta_n^2.\quad (32)$$

It appears that we may have made life more difficult for ourselves, because even when we substitute a finite sum on the left of (32) we must still evaluate an infinite sum on the right. However, note that since the terms in the sum are positive,

$$\left\| \sum_{n=0}^{\infty} \epsilon_n h_n \right\|^2 \geq \sum_{n=0}^N \beta_n^2,\quad (33)$$

where the sum on the right is always finite and is in terms of a finite length error sequence $(\epsilon_0, \dots, \epsilon_N)$. Hence,

$$d_{\min}^2 \geq \min_{\substack{\epsilon_1, \dots, \epsilon_N \\ \epsilon_0 = 1}} \sum_{n=0}^N \beta_n^2\quad (34)$$

and, furthermore, the right side of (34) approaches the left side monotonically as $N \rightarrow \infty$.

The minimization of (34) is no more or less difficult to perform than that of the direct minimization of (12). It does require the existence of a DFE and evaluation of the coefficients $\{C_m\}$. A reasonable procedure is, at each stage of N , to minimize the right side of (34) to obtain a lower bound on d_{\min}^2 and substitute the minimizing sequence into (12) to obtain the upper bound* on d_{\min}^2 . When the lower and upper bounds are sufficiently close, the process can be terminated.

* Note that any sequence substituted into (12) yields an upper bound on d_{\min}^2 , and the one which minimizes (34) is as good as any. On the other hand, only the sequence which minimizes (34) yields a valid lower bound, so it must be minimized.

The minimization of (34) can be assisted slightly by dynamic programming. Defining

$$f_{N-m}(\epsilon_1, \dots, \epsilon_{m-1}) = \min_{\epsilon_m, \dots, \epsilon_N} \sum_{n=m}^N \beta_n^2, \quad (35)$$

we note that

$$\min_{\epsilon_1, \dots, \epsilon_N} \sum_{n=1}^N \beta_n^2 = \min_{\epsilon_1} [f_{N-2}(\epsilon_1) + \beta_1^2] \quad (36)$$

with a recursion relation for $f_{N-m}(\epsilon_1, \dots, \epsilon_{m-1})$,

$$\begin{aligned} f_{N-m+1}(\epsilon_1, \dots, \epsilon_{m-2}) &= \min_{\epsilon_{m-1}, \dots, \epsilon_N} \sum_{n=m-1}^N \beta_n^2 \\ &= \min_{\epsilon_{m-1}} \left[\min_{\epsilon_m, \dots, \epsilon_N} \sum_{n=m}^N \beta_n^2 + \beta_{m-1}^2 \right] \\ &= \min_{\epsilon_{m-1}} [f_{N-m}(\epsilon_1 \dots \epsilon_{m-1}) + \beta_{m-1}^2]. \end{aligned} \quad (37)$$

Because there is no possibility of using forward dynamic programming in this case, the savings in computation for this method is not too spectacular. Each β_n must still be evaluated for 3^N error sequences; the savings is in eliminating the need for summing β_n^2 for most of the combinations of 3^N error sequences.

We note in passing that using the FFT algorithm to reduce the computational effort in the convolutional sum of (31) is a possibility. However, the 3^N sequences for which it must be evaluated becomes a limiting factor long before the savings of that method becomes substantial.

In the foregoing discussion, the existence of a DFE has been required [that is, $\|e_0^+\| > 0$ or equivalently $\log R(\omega)$ is integrable, where $R(\omega)$ is the equivalent power spectrum of the channel¹]. When $\log R(\omega)$ is not integrable (as when it vanishes on an interval), there does not appear to exist an expansion of the type (31) to (32). What can be done is to use the Gram-Schmidt expansion of the form

$$h_m = \sum_{k=0}^m \langle h_m, w_k \rangle w_k, \quad (38)$$

where w_k is the orthonormal sequence obtained from $\{h_k\}$ by the usual Gram-Schmidt orthonormalization procedure. This expansion merely requires that $\{h_k\}$ be linearly independent, which is guaranteed by the existence of an interval on which $R(\omega)$ does not vanish.¹ From (38), it

follows that

$$\begin{aligned} \sum_{m=0}^{\infty} \epsilon_m h_m &= \sum_{m=0}^{\infty} \epsilon_m \sum_{k=0}^m \langle h_m, w_k \rangle w_k \\ &= \sum_{k=0}^{\infty} \beta_k w_k \end{aligned} \quad (39)$$

$$\beta_k = \sum_{m=k}^{\infty} \epsilon_m \langle h_m, w_k \rangle. \quad (40)$$

The key point is that the summation in (40) is infinite, so that evaluation of the lower bound of (34) is now necessarily over infinite error sequences. The finite sum in (31) results from the form of the expansion (7) in which h_n is expanded in terms of all future w_k 's, and this expansion is in turn dependent on h_n not being an element of $M(h_k, k > n)$. Thus, when a DFE does not exist there appears to be no alternative to evaluating a sequence of upper bounds to d_{\min}^2 obtained by a finite sum approximation without the benefit of lower bounds to measure the degree of convergence.

III. THE PERFORMANCE OF THREE RECEIVERS ON THE \sqrt{f} CHANNEL

Results of a calculation of the performance of the MLD, DFE, and ZFE will now be reported for the \sqrt{f} channel, for which the attenuation in decibels increases as the square root of frequency. The \sqrt{f} channel is a good approximation to coaxial cable, as well as to some cables consisting of wire pairs, and for this reason it is of great practical interest.

Many present high-speed digital transmission systems use some form of linear equalization, and their performance will be reasonably well approximated by that of the ZFE. Thus, the comparison between the ZFE and the MLD gives us an indication of the size of the gap in performance between common transmission systems in use today and what could theoretically be achieved by much more complex receiver designs.* The comparison with the DFE is much less interesting, because the susceptibility of the DFE to decision errors is not included in the present analysis and, as will be shown shortly, is of such a magnitude on the \sqrt{f} channel as to essentially invalidate the performance estimate we calculate.

* This comparison is, of course, very idealized. The only impairment we consider is additive Gaussian noise.

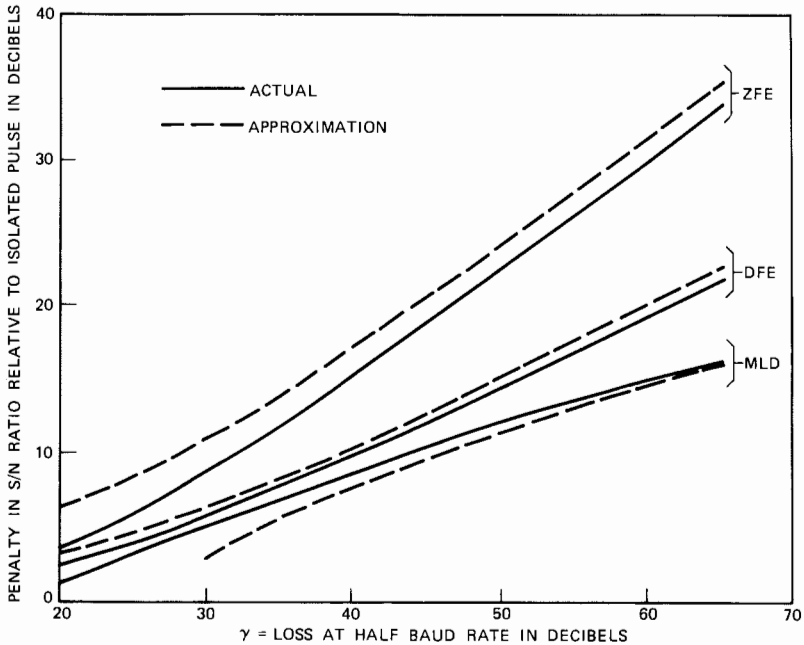


Fig. 2—Performance of three receivers on the \sqrt{f} channel.

The power spectrum of the \sqrt{f} channel is given by

$$|H(\omega)|^2 = 2\pi K^2 R_0 e^{-2K\sqrt{\omega}}, \tag{41}$$

where $H(\omega)$ is the frequency response of the channel and K is a parameter proportional to the line length. The usual convention is to designate the loss at the half-baud rate ($\omega = \pi/T$),

$$\gamma = -10 \log \frac{|H\left(\frac{\pi}{T}\right)|^2}{|H(0)|^2} \text{ (dB)}, \tag{42}$$

in which case

$$K = \sqrt{\frac{T}{\pi}} \frac{\gamma}{20 \log e}. \tag{43}$$

The effective penalties in S/N ratio relative to the isolated pulse bound can be calculated for the ZFE and DFE using the methods of Ref. 1, and for the MLD using the methods developed in Section II. The result is shown in Fig. 2 for the range of γ of practical interest. Most high-speed transmission systems in use today have a γ less than

about 65 dB because of limitations in the maximum gain which can be incorporated into a repeater without excessive coupling of the output back into the input.

One interesting feature of Fig. 2 is that even the MLD has a substantial S/N ratio penalty (15 dB) on the \sqrt{f} channel. Thus, Forney's statement³ that on most channels intersymbol interference does not have to lead to a significant degradation in performance does not apply to channels with very severe intersymbol interference, such as are commonly used in high-speed transmission systems.

The value of d_{\min}^2 , valid for Fig. 2, as well as many other examples considered by this author and Forney,⁴ is

$$d_{\min}^2 = 2(R_0 - R_1), \quad (44)$$

where R_k is the autocorrelation of the received pulse.* An approximation to (44) valid for large γ is derived in Appendix A and plotted in Fig. 2 as a dotted line. Approximations to the S/N ratio penalty of the ZFE and DFE are also derived in Appendix A and plotted in Fig. 2. An intuitive interpretation of eq. (44) is given in Appendix B.

As an illustration of the speed of convergence of (34), the sequence of upper and lower bounds is illustrated in Fig. 3 for a \sqrt{f} channel with $\gamma = 60$ dB. These bounds are within 1 dB for $N = 1$ and 0.5 dB for $N = 3$. Thus, convergence is very rapid, even for severe intersymbol interference.

A word of caution is in order with respect to the curve for the DFE in Fig. 2. This curve does not take into account the effect of decision errors on the performance of the receiver. The DFE subtracts, prior to the decision threshold on data digit B_k , the quantity

$$\sum_{m=1}^{\infty} b_m \hat{B}_{k-m}, \quad (45)$$

where \hat{B}_{k-m} is the receiver's previous decision on B_{k-m} and b_m is the tap-gain of the DFE feedback filter. The resulting quantity which is applied to the threshold is¹

$$b_0 B_k + \sum_{m=1}^{\infty} b_m (B_{k-m} - \hat{B}_{k-m}) + n_k, \quad (46)$$

where n_k is a noise sample. Whenever the b_m 's are large with respect to b_0 , a single decision error will likely cause many more errors. The

* This corresponds to the error sequence (1, -1, 0, 0, ...) or, in the notation of Forney, (1 - D).

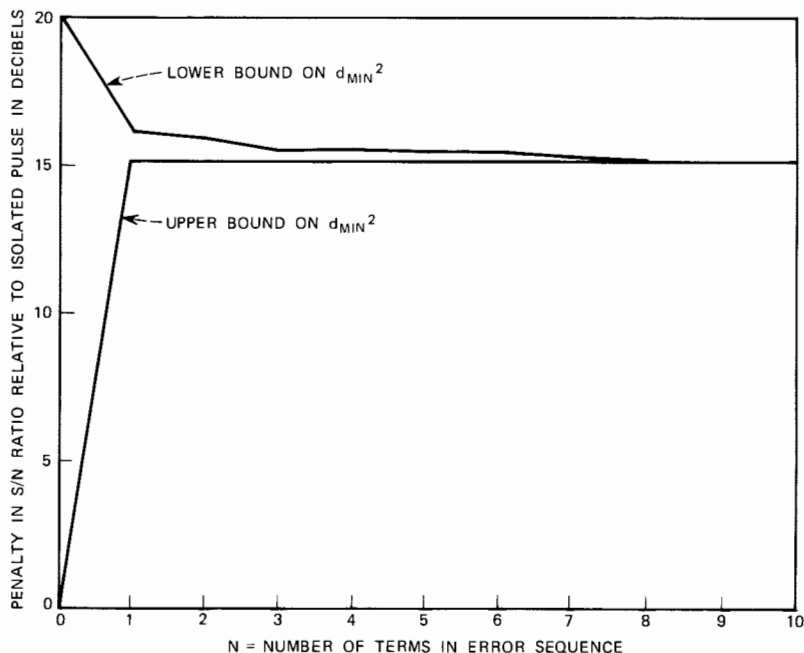


Fig. 3—Convergence of lower and upper bounds on d_{\min}^2 (\sqrt{f} channel with $\gamma = 60$ dB).

coefficients of (46), given by (9), are tabulated in Table I for several values of γ .

Needless to say, the situation is hopeless for the large γ ; the effect of a single decision error will be major and will last for a long time. Even for $\gamma = 20$, the reduction in noise margin resulting from a pre-

TABLE I—COEFFICIENTS OF THE DFE FEEDBACK FILTER (b_m)

m	b_m		
	$\gamma = 20$	$\gamma = 40$	$\gamma = 60$
0	1	1	1
1	0.61	1.4	2.2
2	0.36	1.3	2.8
3	0.25	1.1	2.9
4	0.18	0.94	2.9
5	0.14	0.80	2.8
10	0.06	0.42	1.9
47	0.006	0.06	0.38
174	0.001	0.009	0.06

vious decision error will be significant for five or ten subsequent decisions. We must conclude, then, that Fig. 2 will not be representative of the true performance of the DFE, and further that the DFE may not be a suitable receiver for the \sqrt{f} channel*.

In terms of repeater spacing and baud rate, Fig. 1 can be interpreted in two ways. If the ZFE is replaced by an MLD, the same level of performance can be maintained while either increasing the repeater spacing with a constant baud rate or increasing the baud rate with the same repeater spacing. To illustrate this, consider the example of a ZFE operating at a given level of performance on a \sqrt{f} channel with $\gamma = 40$ dB. Then γ can be increased to 60 dB at the same effective S/N ratio. This corresponds to a 50-percent increase in repeater spacing at a constant baud rate (since γ goes up linearly with the repeater spacing). However, since the repeater spacing has increased, the transmitted power must also be increased by 3.5 dB to maintain a constant isolated pulse energy at the receiver.†

If the repeater spacing is held constant, an increase in baud rate by a factor of $(1.5)^2$, or 125 percent, will also result in a 50-percent increase in γ . Here too, the average (but not peak) transmitted power is increased by 3.5 dB.

The conclusion of these results is that there is a fairly large gap between the performance of linear equalizers and the theoretical limit on the \sqrt{f} channel. It is probably fair to say, however, that practical constraints on repeater complexity, speed of operation, and gain makes the attainment of a substantial portion of this potential improvement on high-speed transmission systems very difficult, at least for the present. Such is not the case for low-speed applications, such as voice-band data, where the implementation of the MLD can be contemplated on the basis of existing technology.

IV. CONCLUSIONS

In this paper, the minimum distance measure has been interpreted geometrically, related to equalization (the decision-feedback equalizer in particular), and bounded in several ways. A practical numerical technique has been developed for calculating the minimum distance without considering unnecessarily long error sequences.

*Tomlinson⁸ has invented a method of avoiding the error propagation problem by subtracting out interference from past data digits in the transmitter.

† The received pulse energy is proportional to γ^{-2} , so that the peak and average transmitted power must be increased by $20 \log(60/40) = 3.5$ dB.

Numerical results for the \sqrt{f} channel reveal that the penalty in S/N ratio relative to the isolated pulse bound for the MLD can be substantial for this channel, and that the gap in performance between the MLD and linear equalization is also substantial. The latter suggests that further attempts at finding receivers without the complexity of the Viterbi algorithm MLD but which nevertheless improve on the performance of linear equalization might well be fruitful. The decision-feedback equalizer does not appear to fit this bill because of its serious error propagation problem when confronted with intersymbol interference as severe as that found on the \sqrt{f} channel.

APPENDIX A

Autocorrelation of the \sqrt{f} Channel

From (41), the autocorrelation is

$$\begin{aligned} R_k &= \frac{1}{\pi} \int_0^\infty |H(\omega)|^2 \cos(\omega kT) d\omega \\ &= \frac{4K^2 R_0}{T} \int_0^\infty x \exp\left(-\frac{2K}{\sqrt{T}} x\right) \cos(kx^2) dx. \end{aligned} \quad (47)$$

Integrating by parts with $u = \exp\left(-\frac{2K}{\sqrt{T}} x\right)$ and $dv = x \cos(kx^2) dx$, we get

$$R_k = \frac{4K^3 R_0}{(kT)^{\frac{3}{2}}} \int_0^\infty \exp\left(-\frac{2K}{\sqrt{kT}} x\right) \sin x^2 dx,$$

which is given in terms of the Fresnel Integral,⁹

$$\begin{aligned} R_k &= \sqrt{\frac{\pi}{2}} \frac{4K^3 R_0}{(kT)^{\frac{3}{2}}} \left\{ \left[\frac{1}{2} - C\left(\frac{K}{\sqrt{kT}} \sqrt{\frac{2}{\pi}}\right) \right] \cos\left(\frac{K^2}{kT}\right) \right. \\ &\quad \left. + \left[\frac{1}{2} - S\left(\frac{K}{kT} \sqrt{\frac{2}{\pi}}\right) \right] \sin\left(\frac{K^2}{kT}\right) \right\}, \end{aligned} \quad (48)$$

where

$$C(x) = \int_0^x \cos\left(\frac{\pi}{2} y^2\right) dy$$

$$S(x) = \int_0^x \sin\left(\frac{\pi}{2} y^2\right) dy.$$

An accurate approximation to R_1 valid for large γ is easily obtained from (47) by substituting the first two terms of a Taylor series for

$\cos x^2$,

$$\begin{aligned} R_1 &\cong \beta^2 R_0 \int_0^\infty x \left(1 - \frac{x^4}{2}\right) e^{-\beta x} dx \\ &= R_0 \left(1 - \frac{60}{\beta^4}\right), \end{aligned} \quad (49)$$

where

$$\beta = \frac{2K}{\sqrt{T}}.$$

Hence

$$2(R_0 - R_1) \cong \frac{120}{\beta^4}$$

and

$$-10 \log \frac{2(R_0 - R_1)}{R_0} \cong 40 \log \gamma - 56.2. \quad (50)$$

Approximations to $\|e_0\|^2$ and $\|e_0^+\|^2$ can also be derived by assuming that $H(\omega) = 0$, $|\omega| > \pi/T$, or equivalently that $|H(\omega)|^2 = R(\omega)$. The resulting S/N ratio penalties are

$$-10 \log \|e_0\|^2/R_0 \cong \gamma + 25.15 - 30 \log \gamma \quad (51)$$

$$-10 \log \|e_0^+\|^2/R_0 \cong \frac{2}{3}\gamma + 15.76 - 20 \log \gamma. \quad (52)$$

Equations (50) to (52) are plotted in Fig. 2 as dotted lines.

APPENDIX B

Interpretation of Equation (44)

It is straightforward to show that whenever

$$\frac{R_1}{R_0} \geq 0.5 \quad (53)$$

we have

$$d_{\min}^2 \leq 2(R_0 - R_1) \leq R_0. \quad (54)$$

Noting that

$$\begin{aligned} R_1 &= \langle h_0, h_1 \rangle = \|h_0\| \|h_1\| \cos \theta \\ &= R_0 \cos \theta, \end{aligned}$$

where θ is the angle between h_0 and h_1 , eq. (53) becomes

$$\theta \leq 60^\circ. \quad (55)$$

The geometric interpretation of (55) is shown in Fig. 4, where it is seen that (54) is satisfied until $\theta = 60^\circ$, when the triangles become

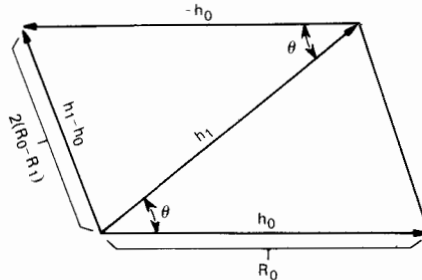


Fig. 4—Geometric interpretation of eq. (44).

equilateral. As long as (55) is satisfied, $h_0 - h_1$ is a shorter vector than h_0 .

In the case of the \sqrt{f} channel, R_1/R_0 is very close to unity. Thus, $h_0 - h_1$ is a very short vector. Although it will certainly not always be the case, a plausible explanation for the fact that longer error sequences do not yet yield a shorter vector is that the addition of other translates of h_k (such as $\pm h_2$) adds further components in other dimensions. Presuming that it does not reduce the component in the $h_0 - h_1$ plane, it can then only increase the length of the total vector.

REFERENCES

1. Messerschmitt, D. G., "A Geometric Theory of Intersymbol Interference. Part I: Zero-Forcing and Decision-Feedback Equalization," B.S.T.J., this issue, pp. 1483-1519.
2. Forney, G. D., Jr., "Maximum-Likelihood Sequence Estimation of Digital Sequences in the Presence of Intersymbol Interference," IEEE Trans. Inform. Theory, *IT-18*, May 1972, p. 363.
3. Forney, G. D., Jr., "The Viterbi Algorithm," Proc. IEEE, *61*, March 1973, p. 268.
4. Forney, G. D., Jr., "Lower Bounds on Error Probability in the Presence of Large Intersymbol Interference," IEEE Trans. Commun., *COM-20*, February 1972, p. 76.
5. Messerschmitt, D. G., "A Unified Geometric Theory of Zero-Forcing and Decision-Feedback Equalization," 1973 Int. Conf. Commun., Seattle, June 1973.
6. Price, R., "Nonlinearly Feedback-Equalized PAM vs. Capacity for Noisy Filter Channels," 1972 Int. Conf. Commun., Philadelphia, June 1972.
7. Grenander, U., and Szego, G., *Toeplitz Forms and Their Applications*, Berkeley: University of California Press, 1958.
8. Tomlinson, M., "New Automatic Equalizer Employing Modulus Arithmetic," Elec. Letters, *7*, March 1971, p. 138.
9. Abramowitz, M., and Stegun, I. A., *Handbook of Mathematical Functions*, New York: Dover, 1965.